Inundation prediction in tropical wetlands from *JULES-CaMa-Flood* global land surface simulations

Toby R. Marthews[1], Simon J. Dadson[1,2], Douglas B. Clark[1], Eleanor M. Blyth[1], Garry D. Hayman[1], Dai Yamazaki[3], Olivia R. E. Becher[2], Alberto Martínez-de la Torre[1,4], Catherine Prigent[5], Carlos Jiménez[6]

[1]UK Centre for Ecology and Hydrology (UKCEH), Maclean Building, Wallingford OX10 8BB, U.K.
[2]School of Geography and the Environment, University of Oxford, South Parks Road, Oxford OX1 3QY, U.K.
[3]Institute of Industrial Science, University of Tokyo, 4 Chome-6-1 Komaba, Meguro City, Tokyo 153-8505, Japan
[4]Meteorological Surveillance and Forecasting Group, DT Catalonia, Agencia Estatal de Meteorología (AEMET), Barcelona, Spain
[5]CNRS, Laboratoire d'Etude du Rayonnement et de la Matière en Astrophysique et Atmosphères (LERMA), Observatoire de Paris, 61 avenue de l'Observatoire, 75014 Paris, France
[6]Estellus, 93 Boulevard de Sébastopol, 75002 Paris, France

Correspondence to: Toby R. Marthews (tobmar@ceh.ac.uk)

Competing interests

The authors declare that they have no conflict of interest.

Abstract. Wetlands play a key role in hydrological and biogeochemical cycles and provide multiple ecosystem services to society. However, reliable data on the extent of global inundated areas and the magnitude of their contribution to local hydrological dynamics remain surprisingly uncertain. Global hydrological models and Land Surface Models (LSMs) include only the most major inundation sources and mechanisms, therefore quantifying the uncertainties in available data sources remains a challenge. We address these problems by taking a leading global data product on inundation extents (*GIEMS*) and matching against predictions from a global hydrodynamic model (*CaMa-Flood*) driven by runoff data generated by a land surface model (*JULES*). The ability of the model to reproduce patterns and dynamics showed by the observational product is assessed in a number of case studies across the tropics, which show that it performs well in large wetland regions, with a good match between corresponding seasonal cycles. At finer spatial scale, we found that water inputs (e.g. groundwater inflow to wetland) became underestimated in comparison to water outputs (e.g. infiltration and evaporation from wetland) in some wetlands (e.g. Sudd, Tonlé Sap) and the opposite occurred in others (e.g. Okavango) in our model predictions. We also found evidence for an underestimation of low levels of inundation in our satellite-based inundation data (approx. 10% of total inundation may not be recorded). Additionally, some wetlands display a clear spatial displacement between observed and simulated inundation as a result of over- or under-estimation of overbank flooding upstream. This study provides timely information on inherent biases in inundation data that can contribute to our current ability to make critical predictions of inundation events at both regional and global levels.

1 Introduction

Wetlands and other inundated areas make up 6-8% of the terrestrial ice-free land surface (Mitsch and Gosselink, 2000, 2015; Junk et al., 2013). However, this percentage greatly underestimates their importance to the global climate system (Wmo, 2019) and to human society (Mitsch and Gosselink, 2000). Wetlands, including peatlands (bogs and fens), mineral soil wetlands (swamps and marshes) and seasonal or permanent floodplains, play a key role in hydrological and biogeochemical cycles, are home to a large part of global biodiversity and provide value to human society in the form of multiple ecosystem services (Junk et al., 2013). Most significantly, wetlands and other inundated areas:

(i) Provide a spectrum of ecosystem services to human society including filtering of pollutants, maintenance of buffers against flood damage, reduction of soil erosion, biodiversity protection and recreational opportunities (Mitsch and Gosselink, 2015; Junk et al., 2013; Maltby and Barker, 2009);

(ii) Are the most significant natural source of atmospheric methane (CH_4), contributing 20-31% of global emissions of this highly potent greenhouse gas (Saunois et al., 2020)

and (iii) Mediate latent heat exchange between the atmosphere and the land surface, thereby greatly affecting the occurrence of deep convection and meso-scale precipitation systems (Taylor, 2010; Prigent et al., 2011; Taylor et al., 2018), with implications for the availability of freshwater resources (Wmo, 2019).

1.1 Inundation extent

Inundation extent is a key impact variable related to wetland dynamics produced by hydrological models, which is calculated from a sequence of water balance calculations carried out over the course of the water cycle (at canopy level, ground level, etc.) (Hewlett, 1982; Sutcliffe, 2004). Precipitation received at the land surface is divided at the top of any vegetation canopy (canopy interception, dividing into canopy storage, throughfall and canopy evapotranspiration, e.g. Best et al. (2011)) and then again at the ground surface (dividing into infiltration (to soil water and drainage into groundwater), soil evaporation, surface ponding and runoff). Heavy or persistent precipitation events may cause *surface water (pluvial) flooding* (= high levels of surface ponding or increased lateral displacement), resulting in higher runoff into local water courses. Once contained in water channels, most water flows along the river network to the ocean (*river routing*), but high river flows may exceed channel capacity downstream, producing an areal extent of inundated water (*overbank inundation*). Land surface inundation, if it occurs, is greater or lesser as a result of a balance between all of these factors.

Globally, we consider wetlands defined in the widest sense of any permanently or temporarily inundated area outside permanent water bodies (Ramsar, 2016). Wetlands may be divided according to their hydrotopographical context (Wheeler and Shaw, 1995) into *groundwater-maintained* or *groundwater-fed wetlands*, where the effects of groundwater dominate over other processes (e.g. fens, the *depressional wetlands* of Usepa (2002), the *non-flooded wetlands* of Miguez-Macho and Fan (2012) or the *groundwater-dependent wetlands* of Froend et al. (2016)), and *fluvial inundation-maintained wetlands*, where

their existence depends primarily on their proximity to a water course that regularly overtops its banks (e.g. igapó and várzea forests of the Brazilian Amazon, Pires and Prance (1985)). Seasonally-varying levels of inundation are primarily dependent on upstream precipitation and how this translates into these two forms of inflow, and secondarily on the ambient rates of evaporation and infiltration (Marthews et al., 2019; Clark et al., 2015; D'orgeval et al., 2008). Further classification of wetlands in terms of vegetation or substrate is not required for our study (but see Wheeler and Shaw (1995), Usepa (2002), Gerbeaux et al. (2018) and Ramsar (2016)). The characterisation of the variation of inundation as a result of the cycles and variability of all these processes is the primary challenge in simulating and predicting inundation (Yamazaki et al., 2011).

1.2 Uncertainty in observations

Much of the uncertainty in the magnitude of important fluxes related to wetlands, is attributable to the wide range of estimates of global inundated areas (Parker et al., in prep. 2020; Aires et al., 2018; Melton et al., 2013; Tootchi et al., 2019; Pham-Duc et al., 2017; Hu et al., 2017). The importance of reducing this uncertainty has long been known from the perspective of policymakers concerned with implementing natural flood management plans (Dadson et al., 2017; Moomaw et al., 2018; Junk et al., 2013) or working in regions where water resources are under threat (Mitsch and Gosselink, 2000; Vörösmarty et al., 2010), but over the last decade this has additionally been recognised more widely in the scientific community in terms of predictions of climate change (Zhao et al., 2017; Thirel et al., 2015). Unfortunately, progress has been relatively slow because of the challenge of simultaneously improving both our observations and our predictions of global inundation extents.

Assessing the precise extent of natural wetlands and other inundated areas from remote sensing remains challenging across large regions (Dutra et al., 2015), especially in the context of constraining process models that produce estimates of wetland extent (see discussion in Saunois et al. (2020)). Observational uncertainty depends on the form of inundation (e.g. deep *vs.* shallow, colder *vs.* warmer water) and ambient conditions (e.g. flooding occurring during a storm under cloud cover *vs.* from snowmelt under clear conditions, or occurring during night *vs.* day hours). Additionally, there are the more general uncertainties in remote sensing products stemming from thresholding assumptions and/or compositing (e.g. see Liang and Liu (2020)). Uncertainty in inundation extent observations continues to be an issue in any study based on remote sensing data, e.g. this uncertainty has recently been shown to be the most significant factor in global CH_4 budget uncertainty (Parker et al., in prep. 2020).

1.3 Uncertainty in model predictions

Many hydrologic models exist that are capable of simulating flood inundation, however these models differ greatly in their sophistication, the breadth of water cycle processes included and their optimal scale of application (Dutta et al., 2000; Beck et al., 2017; Clark et al., 2015; Davison et al., 2016; Clark et al., 2017). Inundation models seldom include all forms of inundation and hydrological processes (Davison et al., 2016; Clark et al., 2015), and the absence of even one process can lead to significant underestimation of inundation extent (e.g. as found by Parker et al. (2018) for the process of overbank inundation). The storage and conveyance of water in lakes, floodplains, groundwater and river channels, especially, is generally simulated only with

relatively high uncertainty in the current generation of land surface models (LSMs) (Marthews et al., 2020; Marthews et al., 2019).

Most hydrological models are run uncoupled from the atmosphere and are therefore reliant on the availability of high-quality precipitation and other atmospheric driving data obtained from independent sources. Uncertainties in the precipitation driving data may often be very significant and larger than the total uncertainty inherent within the model being run (Marthews et al., 2020). Previous studies have attempted to validate global hydrology models against global hydrology products (e.g. Beck et al. (2017) based on the global Water Resources Reanalysis Tier 1 *WRR1* configuration (see Schellekens et al. (2017), now updated to Tier 2 *WRR2* by Fink and Martínez-De La Torre (2017)) and also see (Stacke and Hagemann, 2012; Sterk et al., 2020; Decharme et al., 2012; Yamazaki et al., 2011)). However, many such studies evaluated only runoff or river flow against corresponding models (e.g. Zhao et al. (2017)), without consideration of the areal extent of inundation as we have done in this study.

1.4 Model and study area selection

The global flood simulation model *CaMa-Flood* (Catchment-based Macro-scale Floodplain) was selected for our predictions of inundation extents because of its sophistication and the fact that it is already widely-used (Hoch and Trigg, 2019; Zhao et al., 2017). *CaMa-Flood* is the only open-source global river routing model that is based on the local inertial approximation of the Saint Venant equations (Bates et al., 2010; Dutta et al., 2000; Yamazaki et al., 2013; Fassoni-Andrade et al., 2018), which takes into account the backwater effects of downstream elements, i.e. the possible reversal of flow in particular reaches upstream from e.g. lakes, tributaries, estuaries (Hidayat et al., 2011). By including these effects, *CaMa-Flood* is able to produce a much better characterisation of many wetlands whose dynamics are dominated by surface water inundation.

CaMa-Flood requires runoff data for its simulations, which we obtained from runs of the UK land surface model *JULES* (*Joint UK Land Environment Simulator*) carried out previously through the EU *eartH2Observe* project (Schellekens et al., 2017; Sterk et al., 2020). We chose to use this *JULES*-based dataset because uncertainty in water cycle quantities for *JULES* were comparable to any other equivalent land surface model (Marthews et al., 2020) and because streamflow and runoff data produced by this model have already been validated at regional (Martínez-De La Torre et al., 2019) and global (Arduini et al., 2017) levels. Additionally, through using these models, our results can contribute to the current effort to include global flood inundation in the *JULES* model itself (Dadson et al., submitted 2021; Lewis et al., 2019; Lewis et al., 2018).

Our comparison of model and observational data was based on the observed dataset Global Inundation Extent from Multi-Satellites Version 2.0 *GIEMS-2* (Prigent et al., 2020; Prigent et al., 2007). We analysed the whole tropical zone (23.5°S to 23.5°N, excluding small oceanic islands) at a resolution of 0.25° in both latitude and longitude (Fig. 1). We have taken a case study approach (Table 1), where our wetland areas were selected on the basis of being the largest extant global wetlands, with two limitations. Firstly, we avoided regions with significant inundation on frozen and partially-frozen land because *GIEMS* does not account for frozen water and areas with significant snowfall are systematically masked as well (Prigent et al., 2007). Secondly, coastal or tidal wetlands were also avoided because their interactions with the ocean cannot currently be

simulated by *JULES* or *CaMa-Flood*. Because of the preponderance of coastal occurrence across subtropical and temperate wetlands (Gumbricht et al., 2017; Melton et al., 2013), with these two limitations all remaining large wetlands were in the tropical zone (23.5°S to 23.5°N).

145 In this study, we ask the following questions:

(1) How well can the *CaMa-Flood* model, driven by *JULES* runoff data at 0.25° resolution, simulate observed global inundated extents, as given by *GIEMS* satellite-based data?

(2) Can an improved match between observed and predicted inundation be obtained by simple transformations, e.g. removing low/high observed values or adding a constant to all predicted inundation fractions?

150 (3) Are these simple transformations dependent on spatial scale (e.g. regional *vs.* subcontinental)?

Answering these questions will highlight both the strengths and weaknesses of the *JULES-CaMa-Flood* approach to global inundation prediction and indicate possible directions where improvements may be made in modelling predictive capability in global wetlands.

2 Methods

Observed and simulated inundation extents were compared at a global resolution of 0.25° x 0.25° (approximately 25 km x 25 km at the Equator).

2.1 Observed inundation extents

Observational data on monthly global inundation fraction were obtained from the Global Inundation Extent from Multi-Satellites database version 2.0 *GIEMS-2* (Prigent et al., 2020), which is considered to be one of the best, widely-available global products of inundation extents and captures water under vegetation very well (Hu et al., 2017; Pham-Duc et al., 2017). Data were regridded to a regular spatial resolution of 0.25° x 0.25° to enable comparison with model outputs.

GIEMS is mainly derived from passive microwave observations (Special Sensor Microwave/Imager (SSM/I) and SSMIS), with the help of active microwave and visible and near infrared reflectance observations (Advanced Very High Resolution Radiometer (AVHRR)) to eliminate ambiguities in surface water detection and to account for the potential contribution of vegetation (Prigent et al., 2007; Prigent et al., 2020). *GIEMS* can detect inundation of both natural wetland and irrigated agricultural areas. Frozen surfaces are excluded. In unfrozen areas, the accuracy of *GIEMS* has been comprehensively verified (Papa et al., 2006; Papa et al., 2010) and it is a very widely used remote sensing product (e.g. (Zhang et al., 2016; Taylor et al., 2018)), therefore we suggest that it forms an appropriate benchmark dataset for global modelling studies.

2.2 Simulated inundation extents

Model-derived inundation extents were produced by a sequentially executed run of two models referred to here as *JULES-CaMa-Flood*. Firstly, predictions of land surface runoff were obtained from the UK land surface model *JULES* https://jules.jchmr.org/ (Best et al., 2011; Clark et al., 2011) by accessing simulations carried out previously through the EU *eartH2Observe* project (Schellekens et al., 2017; Sterk et al., 2020; Marthews et al., 2020). A validation of these runoff data against Global Runoff Data Centre (*GRDC*) observations is given in Arduini et al. (2017) and a description of the hydrological simulation approach and water balance calculations in *JULES* is given in Martínez-De La Torre et al. (2019) and Blyth et al. (2019).

Secondly, these runoffs were used to drive the flood inundation model *CaMa-Flood* v3.9.6a (version November 2019) (Yamazaki et al., 2011; Yamazaki et al., 2009), to produce predictions of surface inundation at all points. *CaMa-Flood* was run at a sub-daily timestep (timestep 1 min for runs; 1 day for driving data) and then the outputs were averaged to produce monthly data. *CaMa-Flood* was set to calculate river discharges and flow velocities using the local inertial equation along its river network map in order to include backwater effects (Bates et al., 2010; Yamazaki et al., 2013; Yamazaki et al., 2011). In order to compare more easily with observations on a regular grid, our *CaMa-Flood* simulations were in fully grid-based mode rather than using irregularly-shaped catchments (Yamazaki et al., 2009; Yamazaki et al., 2011). *CaMa-Flood*'s options for

bifurcating flows within the model were not activated for these simulations (Yamazaki et al., 2014) because we did not include coastal wetlands in our case studies (only in coastal wetlands would bifurcation occur at a spatial scale greater than our gridcell scale of approximately 25 km) and because we focus on water balance in our analysis (which should be negligibly affected by river braiding and other bifurcations).

2.3 Analysis

The period for which *eartH2Observe* and *GIEMS-2* data overlap is 1992-2014, so we used this period for all our analyses. All post-processing steps were carried out using NetCDF Operator (NCO) tools v.4.4.5 (Zender, 2008) and the statistical language environment R v.4.0.2 (R Core Team, 2020). For the R-based analyses, packages *maps*, *rgeos* (v.0.5-3), *GEOS runtime* (v.3.8.0) and *rgdal* (v.1.5-12) were required.

2.3.1 Evaluation metrics

We applied the two most common efficiency statistics used in the context of river flow analysis: the Nash-Sutcliffe Efficiency (NSE) and Kling-Gupta Efficiency (KGE), both of which measure the alignment between model results and observations (Table 2). KGE is based on a decomposition of NSE into its constitutive components (correlation, variability bias and mean bias) and addresses several perceived shortcomings in NSE (Knoben et al., 2019).

Our focus in this study is wetlands, therefore we excluded areas of very high inundation (permanent lakes and reservoirs, which were always 100% inundated in both observed and simulated data because of substitution from the Global Lakes and Wetlands Database *GLWD* (Lehner and Döll, 2004)) and also areas of continuously low or zero inundation (dry areas in the validation region, which would also provide a constant match between observed and simulated areas, see e.g. (Bernhofen et al., 2018)). Our focus on variability measures ensured that our match statistics were dominated by the regular (seasonal) and irregular cycles occurring at points where inundation was not constant, i.e. wetland regions *sensu stricto*.

2.3.2 Transforming inundation extents

When comparing the observed and simulated inundation extents, it can happen that inundation predicted by *JULES-CaMa-Flood* is not observed by *GIEMS*. Based on the data we have, it is not possible to be certain whether this 'low level' inundation shows some kind of bias towards overprediction on the part of the model, or perhaps the inundation is actually real but for some reason unobserved by *GIEMS* (see e.g. Liang and Liu (2020) for a discussion on the limitations of the satellite-based sensors employed). In order to test this, during our analysis we posit a nonzero, minimum level of inundation fraction *alpha_min* below which *GIEMS* always returns a zero result.

It is also possible that there is a maximum inundated fraction (here called *alpha_max*) above which *GIEMS* loses its sensitivity (i.e. possibly *GIEMS* can differentiate well between 20% and 30% inundation, but not as reliably between 70% and 80%). This may possibly happen because vegetation canopy cover obscures inundation occurring beneath it, and the magnitude of this effect will depend on canopy coverage and the density of the canopy concerned, among other factors (*GIEMS* is capable

of detecting some water under dense vegetation, but with high uncertainty, especially when the distribution of inundation within the gridcell is highly skewed, i.e. small dry areas within a very wet gridcell or *vice versa*) (Prigent et al., 2020).

225   Finally, it may also be the case that our predictions of inundated fraction have a systematic bias (underestimation or overestimation, on a gridcell-by-gridcell basis). In order to test this, we introduce a fraction *beta* which is added to all *CaMa-Flood* outputs of *flooded fraction* (*fldfrc*). In summary, we can modify the *GIEMS* data and *CaMa-Flood* outputs according to the simple transformations in Fig. 2 in order to investigate and quantify bias in both our simulated and observed data.

3 Results

Results are presented in a sequence of case study areas, beginning with the Sudd, Pantanal, Tonlé Sap, Inner Niger Delta and Okavango wetlands before moving to the larger, subcontinental wetland complexes of the Central Amazon and the Congo Cuvette. Straight comparisons between observations and model predictions of inundation show a complicated pattern of partial overlap that is challenging to assess visually (Fig. 3), therefore we calculate appropriate statistics across all case study areas.

3.1 Inundation extent

GIEMS observations and *JULES-CaMa-Flood* predictions match very variably: monthly average inundation extent shows a clear bias in most study wetlands, and in addition there is significant year-on-year variability (Fig. 4). However, the direction of bias is not consistent between wetlands. Nash-Sutcliffe Efficiency (NSE) and Kling-Gupta Efficiency (KGE) scores were calculated for each wetland study area in order to be able to compare consistently the match between simulated and observed wetland and inundation extents. NSE and KGE are metrics based on calculations of error (Normalised root-mean-squared error *RMSE*) and correlation (Pearson's *r* correlation coefficient) (Table 2). We do not report calculated values of RMSE or Pearson's *r* because plots of these statistics contained no information not visible on the corresponding plots of NSE and KGE.

Because of our pixel-based approach, we could apply our NSE and KGE calculations in a distributed way across each case study wetland. These scores are most usually used in relation to discharge data, yielding generally only one time series per catchment (see Suppl. Info), but our inundation estimates at every gridcell enabled us to calculate efficiency on a pixel-by-pixel basis in each of our study areas (Fig. 5). Averaged efficiency scores are generally high across each individual wetland, although lower in parts of the wetlands that have the most dynamic flow regime.

However, NSE and KGE are not capable of measuring some aspects of the flow regime that are important from the point of view of dividing out the different sources of inundation in our study wetlands, most notably spatial displacement of inundation, which might indicate that inundation input is overestimated in one area by the model at the expense of underestimation elsewhere, or alternatively might indicate that inundation inputs have been correctly calculated at all points, but an underestimated flow speed produces inundation at an incorrect location. For example, the Inner Niger Delta wetland shows apparent spatial displacement of inundation between observed and simulated: *GIEMS* reports negligible inundation north of 15.5°N in any month (a result broadly in line with the finer scale analysis of Bergé-Nguyen and Crétaux (2015)) even though *CaMa-Flood* predicts inundation reaching as far as Timbuktu at 16.5°N (Fig. 3). At this spatial resolution, 1° latitude is well- resolved so this is a significant mismatch.

3.2 Identifying an optimal transformation of GIEMS observations and JULES-CaMa-Flood predictions

Varying the values of the three parameters *alpha_min*, *alpha_max* and *beta* (see Fig. 2), we searched for an optimal value of each that brought our observed and simulated data as close together as possible, in order to quantify and therefore help

understand the discrepancy between our model result and the (uncertain) observations. By repeating the calculations that produced Fig. 5 for an exhaustive range of parameter combinations of *alpha_min*, *alpha_max* and *beta*, the state space plots in Fig. 6 were produced. A notably higher value for NSE or KGE for a particular combination of *alpha_min*, *beta* and *alpha_max* identifies a consistent bias in either the model predictions or the observations (or both).

The visible maxima on our state space plots provide a best estimate of the optimal values of these parameters, with these optima differing markedly between our wetland study areas (Fig. 7). We found that *alpha_min* took a nonzero value ~10% across most of our study wetlands (Fig. 7), but found no evidence to suggest that *alpha_max* should consistently take any value <1.0 for any of our wetlands (Fig. 6; i.e. we found no evidence that the *GIEMS-2* inundation extents overestimated inundated fraction in gridcells where inundation covered a large percentage of the spatial cell).

We found high variation in the estimated value of *beta* for each wetland, i.e. adding a consistent constant fraction of inundation extent to all gridcells within the limits of each study wetland did indeed provide a closer match between observations and simulation, at least in the wetlands we considered in this study (Fig. 7). Defining *water_in* = (channel + surface + subsurface inflow + precipitation) and *water_out* = (infiltration + evaporation), we suggest that the negative values of *beta_opt* in the Amazon, Tonlé Sap, Sudd and Inner Niger Delta show probable underestimation of hydrological output by *JULES-CaMa-Flood* (*water_out*) (Fig. 7). Conversely, the positive values of *beta_opt* in the Okavango show probable underestimation of hydrological input by *JULES-CaMa-Flood* (*water_in*) (Fig. 7).

Finally, we note the specificity of our results to the time period 1992-2014. Carrying out this analysis for an earlier or a later period would certainly yield different estimates of NSE, KGE, *alpha_min*, *alpha_max* and *beta*. However, we suggest that without significant climate change, or perhaps significant anthropogenic modification of the wetland area concerned, the values of these statistics should remain similar to the values calculated here.

4 Discussion

There has recently been significant progress in our understanding of wetlands and the roles they play in climate processes, land surface processes and their impacts on human society (Saunois et al., 2020; Ipcc, 2014; Mitsch and Gosselink, 2015;
290   Moomaw et al., 2018). However, even though the physics of flood inundation is relatively well-known (Yamazaki et al., 2013; Bates et al., 2010; Fassoni-Andrade et al., 2018), many hydrological processes relevant to the representation of flooding in Earth system models remain poorly characterised at the high resolutions required to address issues of local and regional impact (Marthews et al., 2019; Zhou et al., in prep. 2020; Bierkens, 2015; Clark et al., 2015), including infiltration (D'orgeval et al., 2008; Clark et al., 2015), and evaporation (Robinson et al., 2017; D'orgeval et al., 2008) of flood waters, as well as groundwater
295   effects (Clark et al., 2015).

In this study, we have simulated inundation extent at a spatial resolution high enough to resolve the major details of most major global wetlands. These results are potentially of great use to a wide audience of academic and non-academic users interested in the broad-scale impacts of environmental change on wetlands, especially where seasonal inundation affects water and energy fluxes in Earth system models. It is therefore appropriate to seek as robust a validation of these predictions as
300   possible.

4.1 Comparing simulated and observed global inundated extents

We found that our simulated inundation extents (from the *CaMa-Flood* model, driven by *JULES* runoff data at 0.25° resolution) sometimes compared very closely to our observed data (from *GIEMS* satellite-based data), but at many points there were
305   divergences (Fig. 3). For example, in the Sudd wetland, our model appears to over-predict inundation, whereas in the Pantanal it appears to under-predict (Fig. 3). Can we explain these and other differences between *GIEMS* observations and our model predictions?

In order to investigate these divergences, we applied simple transformations to our data (Fig. 2) and the optimal values of the three parameters *alpha_min*, *alpha_max* and *beta* we found for each wetland provide robust explanations for observable
310   differences. We found that our predictions of inundation extent could be improved at local or regional scale by simple transformations involving the three parameters *alpha_min*, *alpha_max* and *beta*. Moreover, in what follows we use our diagnosis of these differences to highlight opportunities to improve the representation of physical processes in land-surface and large-scale hydrodynamic models.

We found evidence that *alpha_min* might generally take a nonzero value ~10% across tropical inundated areas,
315   indicating that *GIEMS-2* may be missing widely-distributed occurrences of low inundation within these wetlands, as suggested by previous studies (Prigent et al., 2007). *GIEMS* may underestimate low levels of inundation that occur outside wetlands because of uncertainties in estimating inundation e.g. below intact forest canopies (although small in any particular location, these would sum to a significant missing term in regional and continental water budgets).

We found high variation in the estimated value of *beta* for each wetland, i.e. the constant fraction of inundation extent
that must be added to all gridcells within the limits of each study wetland to elicit the closest match between observations and
simulation. Our interpretation of this is influenced by the consideration that we know the *JULES-CaMa-Flood* model does not
simulate several hydrodynamic processes that are known to have a great impact on inundation extent (e.g. evaporation of
flooded areas). Defining *water_in* = (channel + surface + subsurface inflow + precipitation) and *water_out* = (infiltration +
evaporation), we suggest that some wetlands show underestimation of hydrological output by *JULES-CaMa-Flood*
(*water_out*) (e.g. Amazon, Tonlé Sap, Sudd and Niger Inland Delta), whereas some show underestimation of hydrological
input by *JULES-CaMa-Flood* (*water_in*) (e.g. Okavango). From a basic comparison of observed and modelled inundation
extent, it is not possible to identify the precise combination of climate, season or hydrotopography that produces these under-
and over-estimations of water balance at these particular wetlands, but identifying the sign of the imbalance is nevertheless
very useful information for interpreting model predictions in these areas.

The spatial displacement of inundation prediction downstream from observed inundation visible especially in our
results for the Inner Niger Delta and the Sudd (Fig. 3) is a result of over- or under-estimation of overbank flooding upstream.
If overbank flooding is underestimated in our simulation then the water within the river course (the Niger or White Nile,
respectively, in these cases) will remain in the river and be taken downstream further than expected, producing a downstream
wetland 'extension' that exists in the simulation results but not the observed (as we see in our *JULES-CaMa-Flood* outputs).

4.2 Implications for the hydrodynamic balance of wetlands

Wetlands exist as a balance between water input and water output, (i.e. *water_in* and *water_out* above; a landscape-scale water
balance *sensu* Sutcliffe (2004)). In order to understand these and other points of divergence between observation and
prediction, we need to understand this balance calculation in that particular wetland, and also assess what types of water bodies
are represented in the simulated data (Zhou et al., 2020; Zhou et al., in prep. 2020).

The optimal parameter value derived in this study *beta_opt* may be understood as an index unique to each wetland
that estimates the amount that is missing or underestimated in the overall wetland water balance. For example, *beta_opt* will
be negative if evaporation and infiltration are being significantly underestimated by *JULES-CaMa-Flood* in this study area
(neither *JULES* nor *CaMa-Flood* explicitly models evaporation from inundated water in their present configurations).
Conversely, *beta_opt* will be positive if e.g. groundwater inflow is being underestimated. Therefore, the value of *beta_opt* may
be thought of as an estimate of how much *water_in* is underestimated by *CaMa-Flood* minus how much *water_out* is
underestimated.

Categorising wetlands in terms of positive or negative *beta_opt* would be superficially similar to the division by Junk
et al. (2011) of South American wetlands into *fluvial* (wetlands that are predominantly maintained by river overbank inundation
rather than by groundwater effects) and *interfluvial* wetlands (where groundwater effects dominate), however theirs was a
distinction based on overall water balance rather than the balance of water input. In the context of our analysis here, we
understand fluvial and interfluvial wetlands to mean ones where *water_in* is dominated by channel/surface flow or subsurface

inflow, respectively. Both fluvial and interfluvial wetlands may of course experience high evaporation rates (e.g. the Inner Niger Delta) or high infiltration rates (based on underlying soil type) and therefore may occur either above or below the $y=0$
355 line in Fig. 7.

4.3 Inundation at subcontinental and larger scales

Looking at subcontinental scales (the Amazon and the Congo) and larger scales (the three tropical zones, Fig. 1), a number of additional considerations become more important. As with all very large river basins, the inland reaches of the Amazon and
360 the Congo are collectively enormous wetland complexes, with some areas dominated by river flow and others by topographic factors (e.g. the "cuvette" of the Congo Cuvette indicates the whole subcontinent is approximately a shallow bowl). The same diagnosis of biases may be carried out over these larger areas, but our optimal value for *beta* generally converges closer and closer to the 'null' value *beta*=0.0 as larger and larger regions are considered (at least, for regions that do not include significant coastal or permafrost areas). This is reasonable, because even the largest wetland areas are localised regions at this scale and
365 therefore these optima will be averaged together with an increasing number of relatively *terra firme* gridcells (i.e. gridcells which experience little or no regular inundation) and, at the largest scales, with entire mountain ranges where little or no inundation occurs (either in our model or in the observations).

In addition, we should expect that *beta_opt* should converge to zero at the largest scales because we know that these models return reliable global estimates (Yamazaki et al., 2011), therefore from a global perspective the magnitude of values
370 for a particular wetland or wetland complex should be understood as biases that are balanced out elsewhere. However, wetland-specific values nevertheless provide useful information about the inundation processes that dominate in those particular wetlands and allow us to improve our understanding of landscape-scale and continental-scale inundation hydrodynamics.

4.4 Conclusions

375 Simulations of inundation extent are important because they allow us to predict what will happen to globally-important wetlands in the future. Wetlands are known to be key nodes in the biosphere system in terms of vulnerability to climate change (Maltby and Barker, 2009; Mitsch and Gosselink, 2015). However, wetlands are also highly dynamic landscape-level entities produced by the balance of a number of different water cycle processes acting together (Hewlett, 1982; Sutcliffe, 2004), not all of which are yet represented in global hydrodynamic models (Yamazaki et al., 2013; Yamazaki et al., 2011).

380 Reducing uncertainty in predictions from large-scale inundation models has long been a prerequisite for their use in global Earth system models. In this study we have shown that a very reasonable and close match may be derived between *JULES-CaMa-Flood* model predictions of inundation extent and independent *GIEMS-2* global satellite-based observations of inundation. Differences do occur at regional scale in particular large wetlands, however, and these differences indicate clearly the importance of incorporating into the modelling framework a better representation of the hydrological impacts of, especially,
385 infiltration, evaporation and groundwater-fed inundation. These comments are not only relevant to *GIEMS-2* and *JULES-CaMa-Flood* data: all satellite-based inundation data have biases that may be assumed to be very similar to those inherent in

GIEMS data, and all model predictions of inundation have biases and uncertainties presumably similar to those that are in *JULES-CaMa-Flood* predictions (Dutra et al., 2015; Liang and Liu, 2020; Parker et al., in prep. 2020; Saunois et al., 2020), so we believe that our results and analysis provide a blueprint for users of other model/observational data on how they might

390 assess and account for these types of bias in their own data.

Improving our understanding of the dynamics of inundated areas and the role they play in the generation of land-atmosphere fluxes requires a better representation in general of wetlands within global land-surface and hydrodynamic models (Zhang et al., 2016). The results of this study point clearly towards the need for greater attention to be paid to hydrological dynamics and water cycle processes within these models, which we expect to result in improved modelling predictive

395 capability in global wetlands in the future. A firm focus on producing a better characterisation of hydrodynamics within this class of models will produce enormous positive returns in terms of our global capability to predict inundation and its global impacts and will make a welcome contribution to our preparedness for the impacts of future climate change (Moomaw et al., 2018; Ipcc, 2014).

400

Code/Data Availability

All model data used in these analyses are publicly available via the *eartH2Observe Water Cycle Integrator portal* https://wci.earth2observe.eu/. All code used in our analysis will be made available on request to the corresponding author.

405

Author contribution

TRM, SJD and DBC conceptualized this study in discussion with EMB, GDH and DY. OREB and AMdlT contributed expertise from earlier projects and helped with formal analysis. DY provided expertise on the use of *CaMa-Flood* and CP and CJ provided *GIEMS-2* observational data and expertise on its interpretation. TRM prepared the manuscript with contributions from all co-authors.

410

Acknowledgements

This work was supported by the Natural Environment Research Council through the National Capability *Hydro-JULES* project (grant number NE/S017380/1). TRM thanks colleagues at UKCEH for extremely useful discussions during the development of this paper. This work used *JASMIN*, the U.K.'s collaborative data analysis environment (http://jasmin.ac.uk). GH acknowledges the support of NERC through the grant *The Global Methane Budget, MOYA* (NE/N015746/2)

415
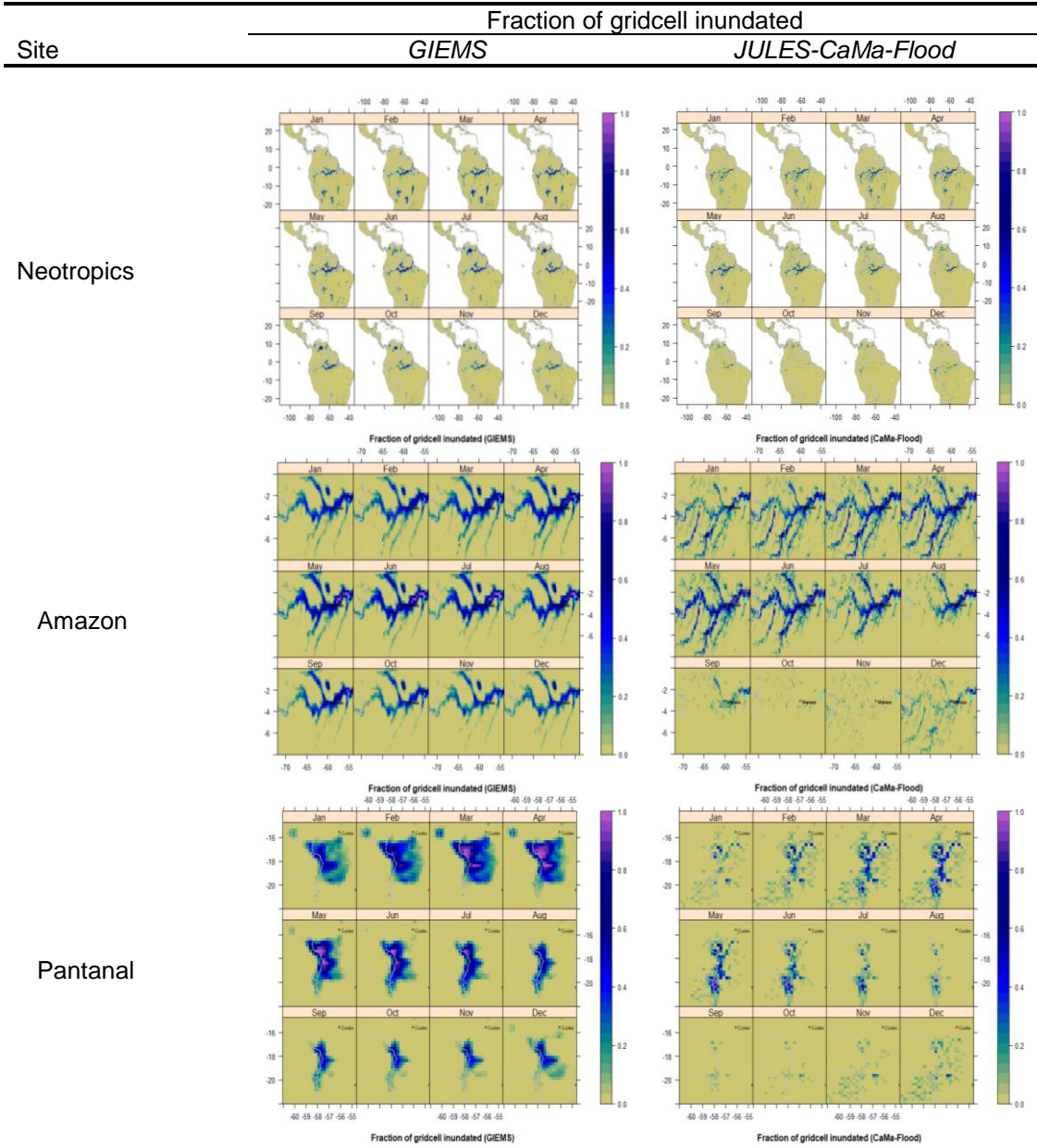
	Fraction of gridcell inundated	
Site	*GIEMS*	*JULES-CaMa-Flood*

West Paleotropics
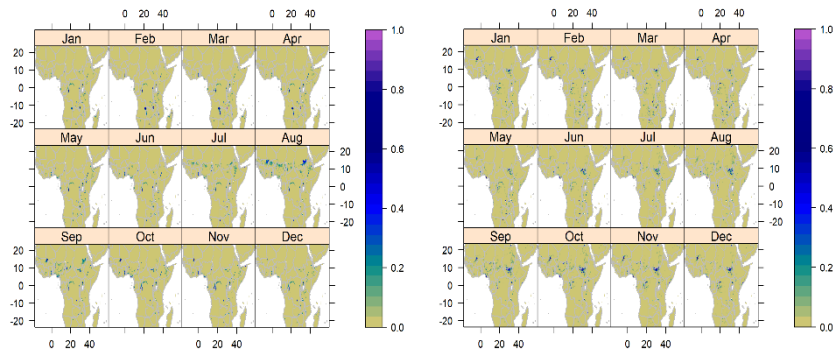
Niger Inland Delta
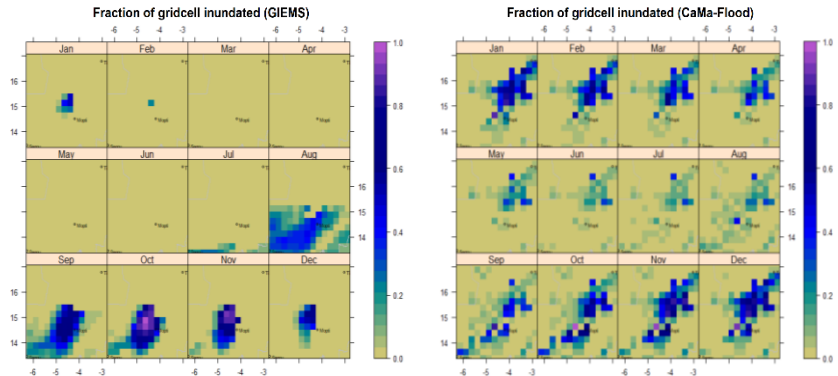
Sudd
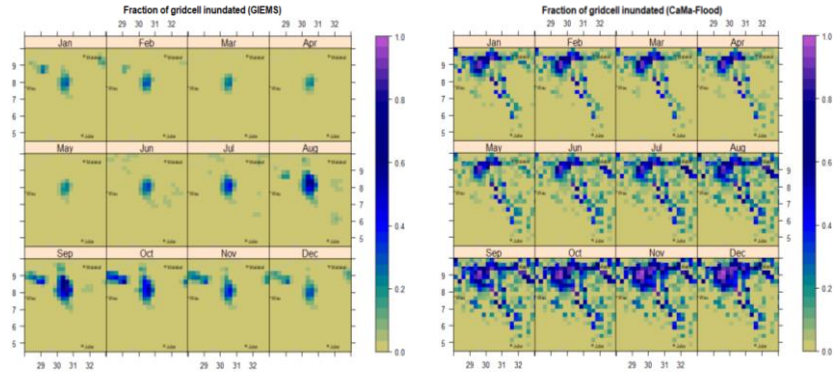
Congo
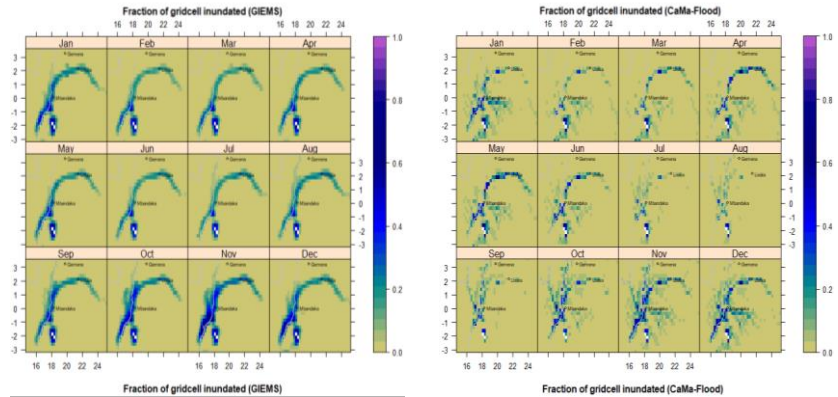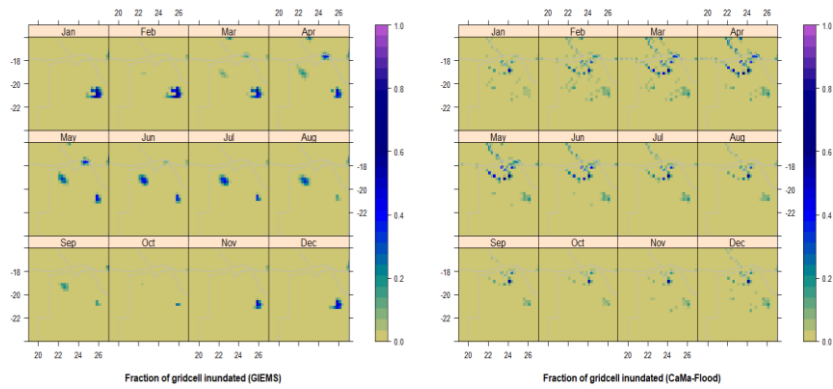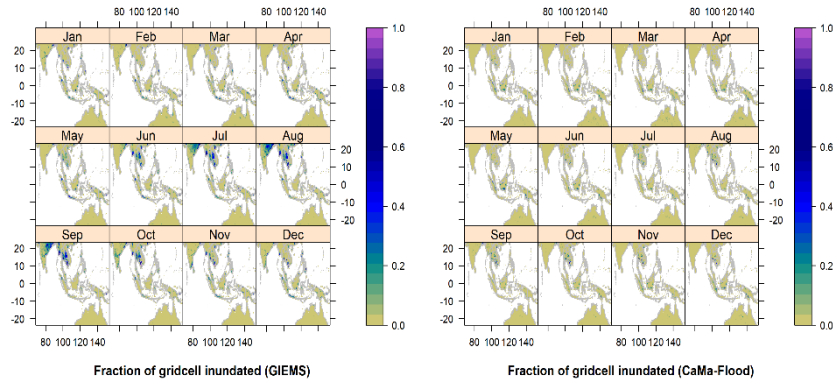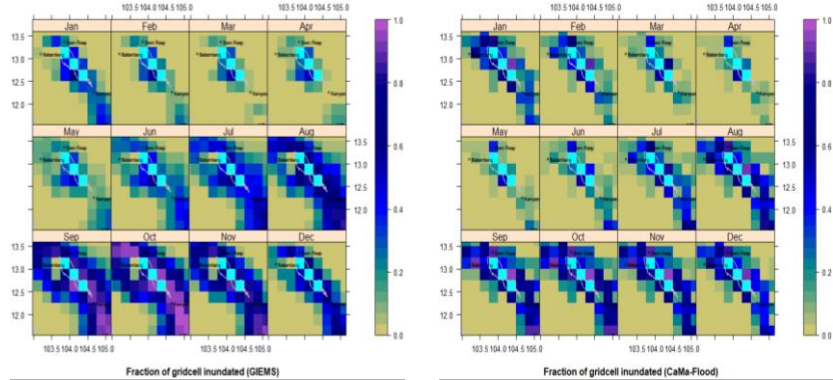
Figure 3: Fraction of gridcell inundated (in addition to water contained in channels and watercourses, which are not shown) in each study area. Superposed lakes and reservoirs are from the Global Lakes and Wetlands Database *GLWD* (Lehner and Döll, 2004). Resolution is 0.25° in both latitude and longitude (n.b. the Tonlé Sap is our smallest wetland, therefore the gridcells are relatively large in that plot). View window extent is taken from references in Table 1. Cities with populations >100 000 are shown **(Simplemaps, 2019)** for view extents up to 2 000 000 km². Data shown are an average for 1992-2014 from *GIEMS-2* observations (left) and equivalent *JULES-CaMa-Flood* simulations (right).

Site	Seasonal variation of inundation (fraction of area)
Amazon	
Pantanal	
Niger Inland Delta	
Sudd	
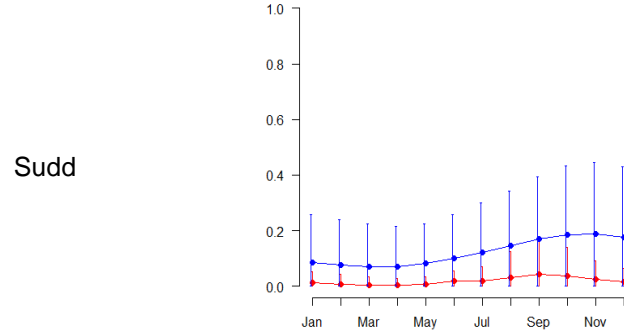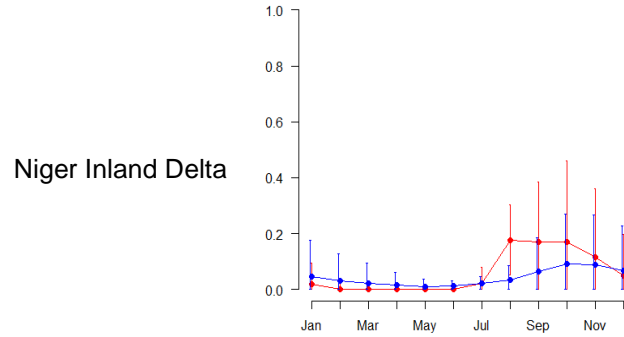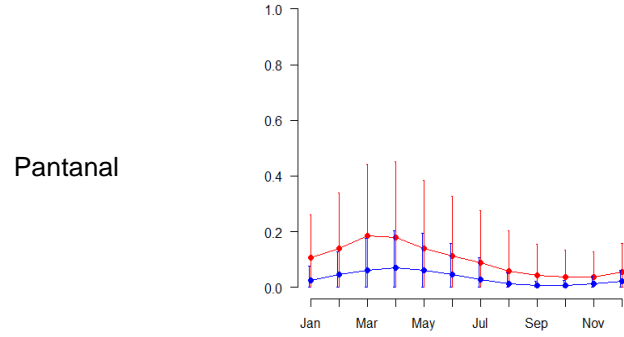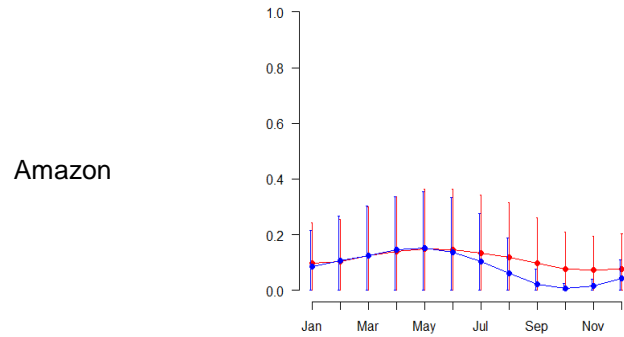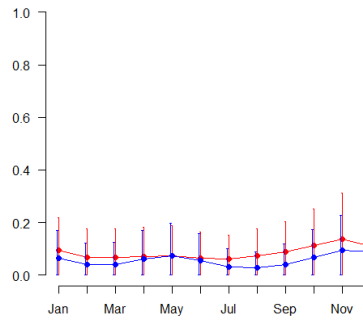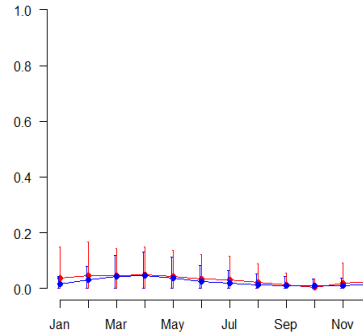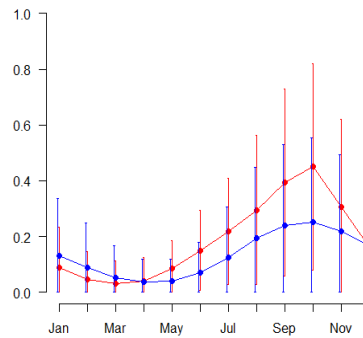
430 **Figure 4**: Seasonal variation in inundation across the study wetlands, averaged across the years 1992-2014: Red = Observations (*GIEMS*), Blue= Simulated (*JULES-CaMa-Flood*). The three main tropical zones are not shown because they include areas both north and south of the Equator.
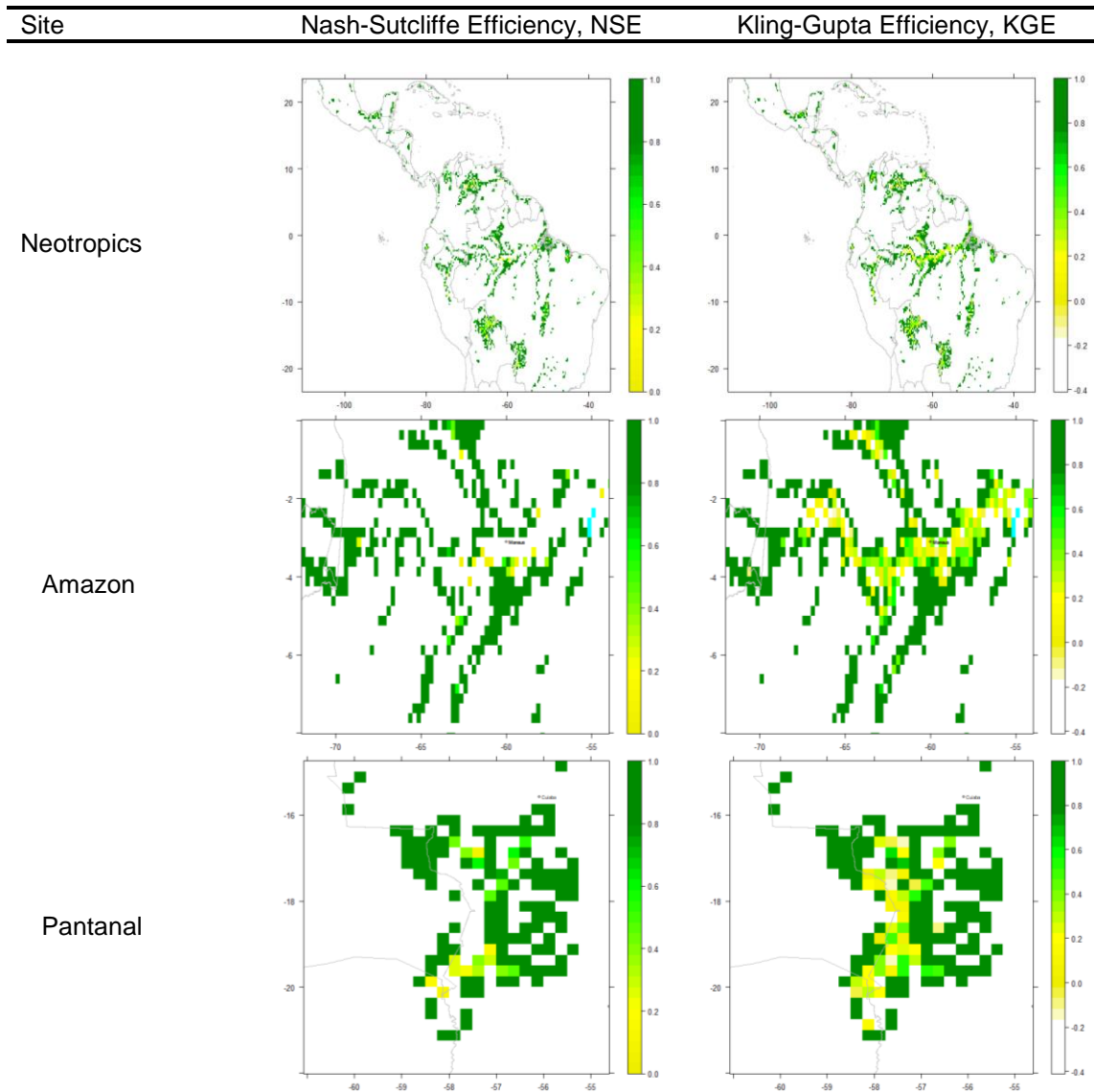
Site	Nash-Sutcliffe Efficiency, NSE	Kling-Gupta Efficiency, KGE
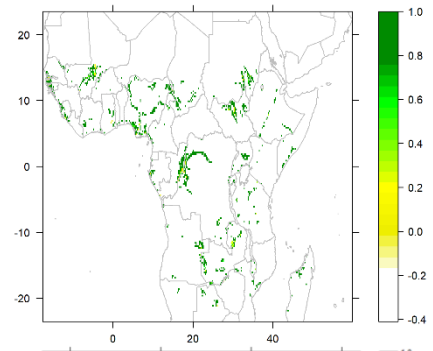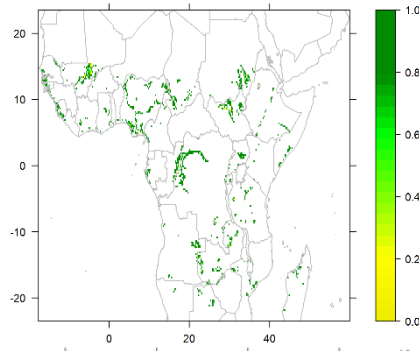
West Paleotropics

Niger Inland Delta
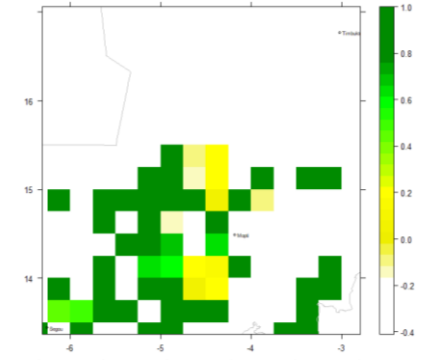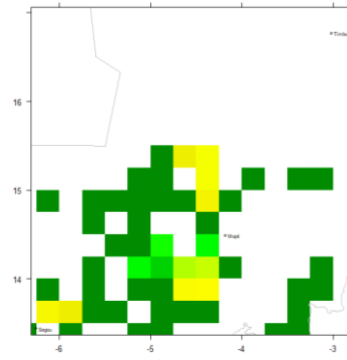
Sudd
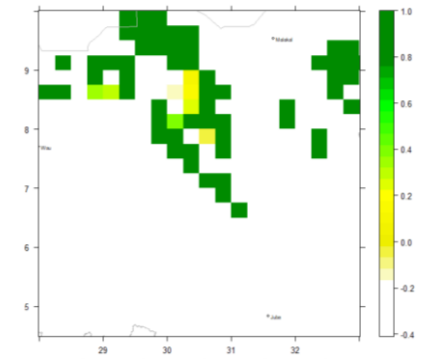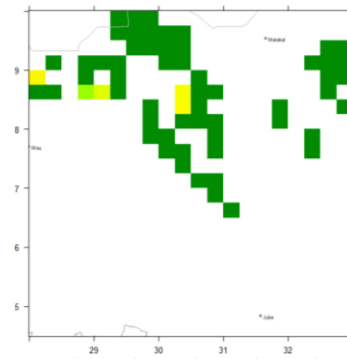
Congo
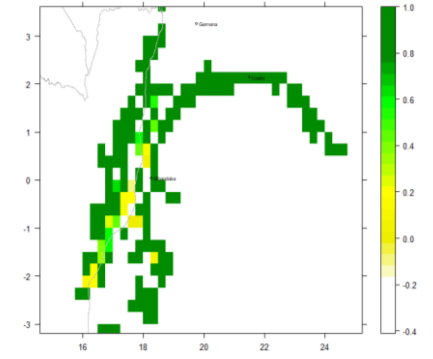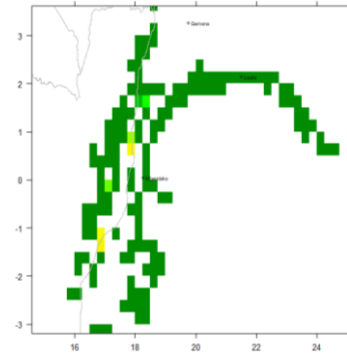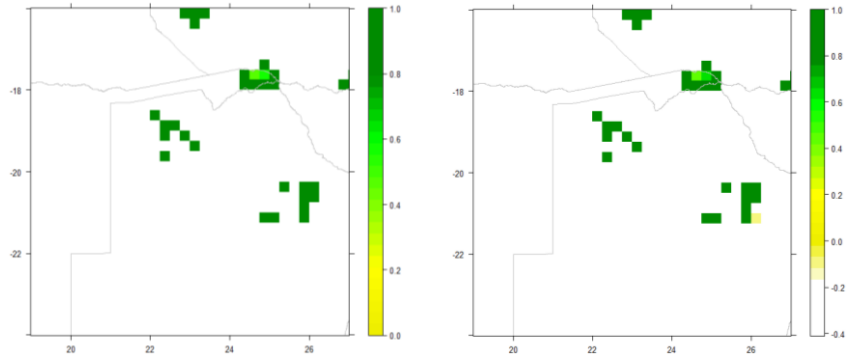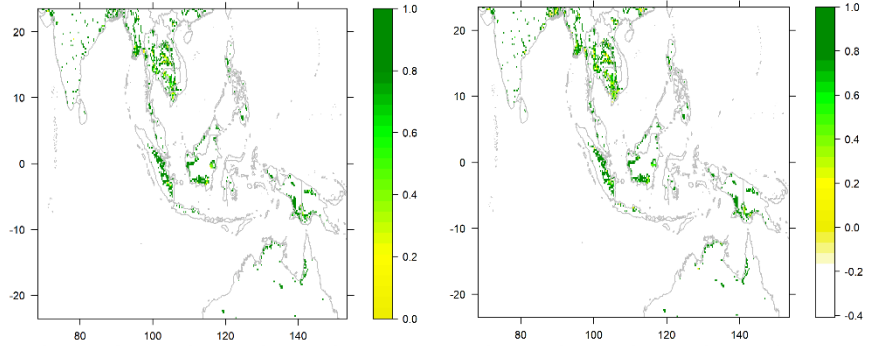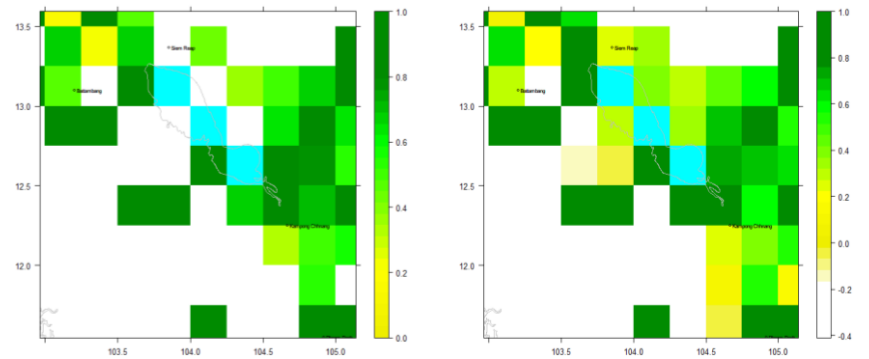
Figure 5: Mapped values for efficiency statistics based on inundated gridcell fraction, averaged across the years 1992-2014 (with *alpha_min*=0.0, *beta*=0.0 and *alpha_max*=1.0) (white indicates no value could be calculated).
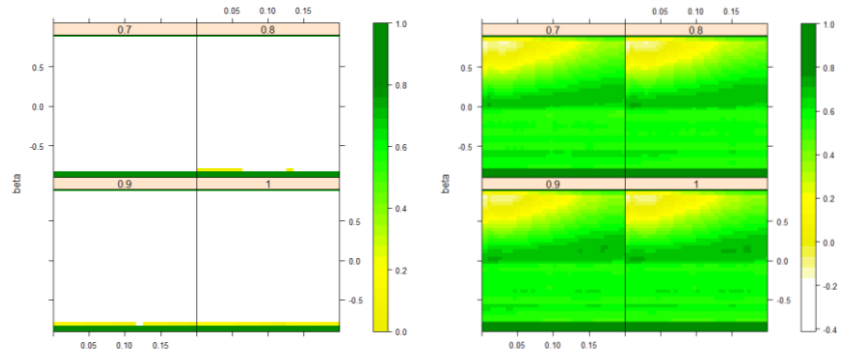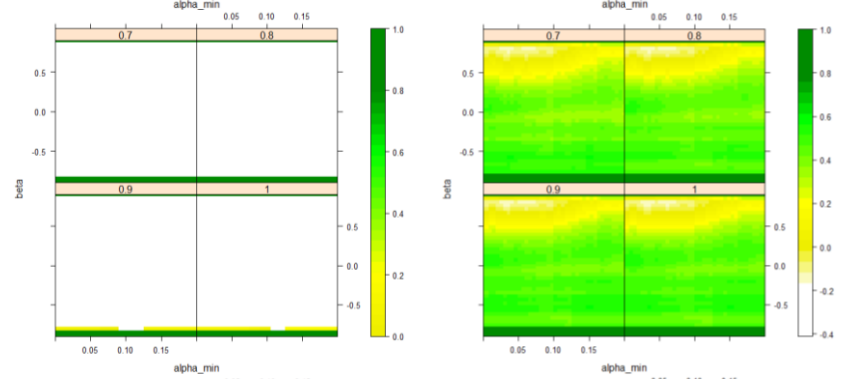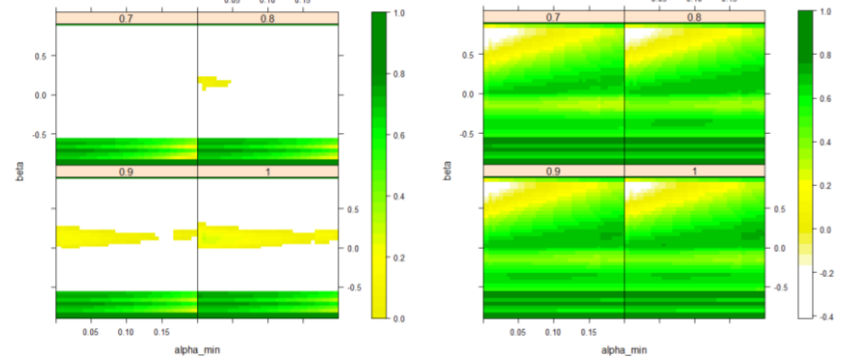
Site	Nash-Sutcliffe Efficiency, NSE	Kling-Gupta Efficiency, KGE
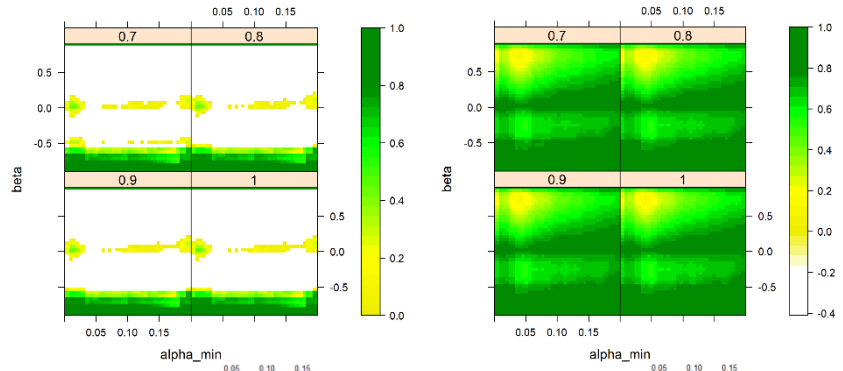
West Paleotropics

Niger Inland Delta
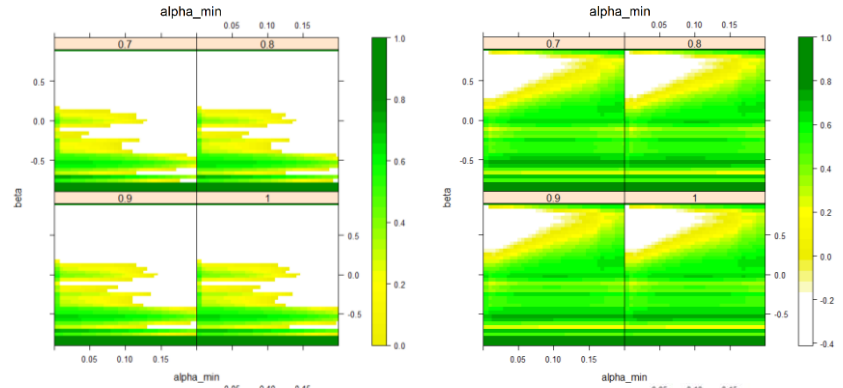
Sudd
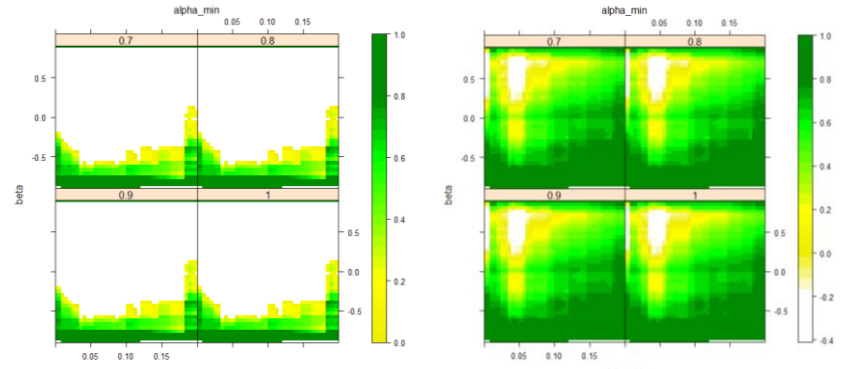
Congo
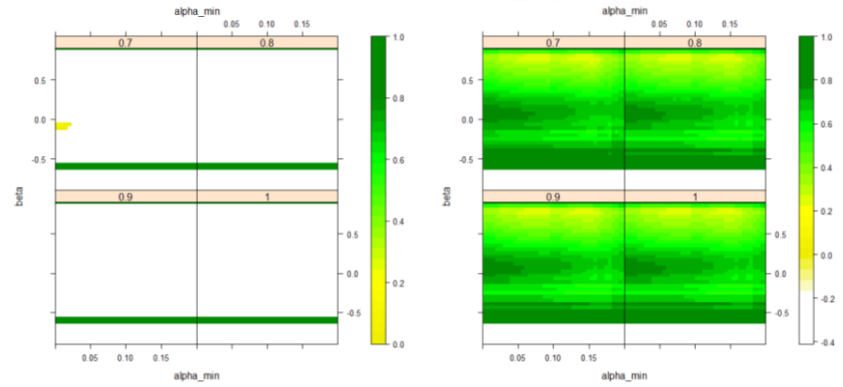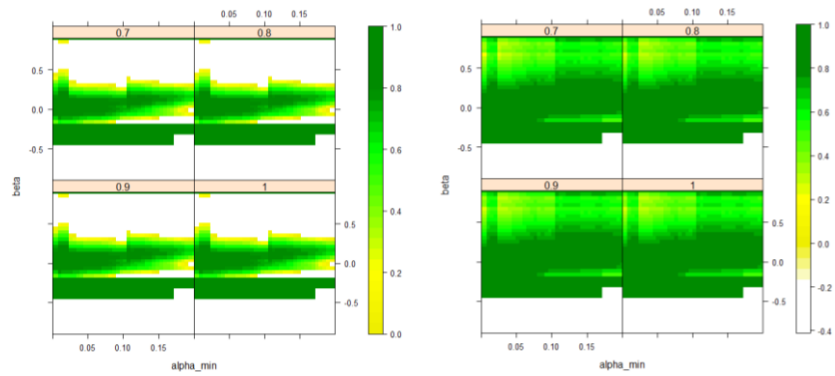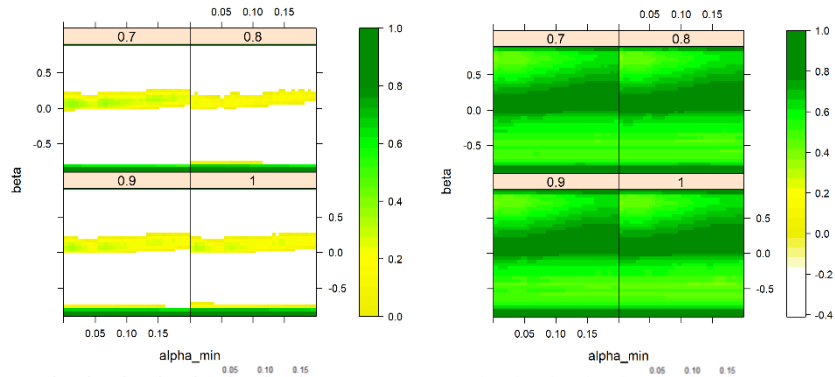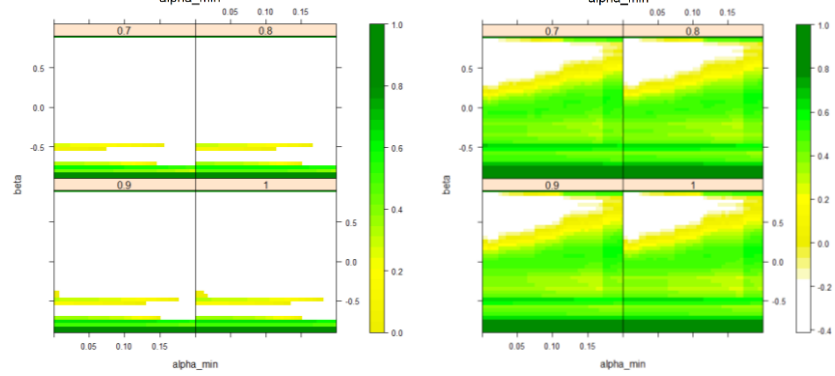
Figure 6: State space plots for evaluation statistics based on inundated gridcell fraction, calculated from varying parameters *alpha_min* and *beta*, with panels showing values of *alpha_max*. Each point is the mean of all NSE or KGE values, averaged both over time (years 1992-2014) and over the wetland region concerned (white indicates no value could be calculated).

445
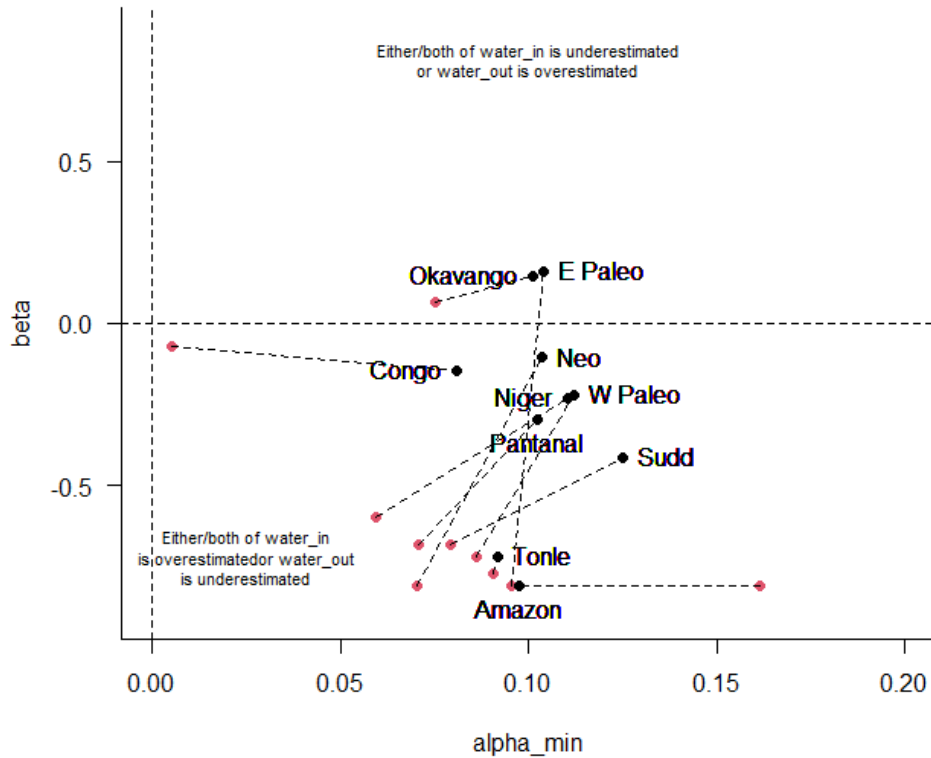
Figure 7: Summary of plots in Fig. 6. Optimal values of *beta* and *alpha_min* are shown (referred to as *beta_opt* and *alpha_min_opt* in the text), calculated as the centroids of the maximal region on the KGE plots (black) or NSE plots (red) for each site (with *alpha_max*=1.0) from Fig. 6. On this plot, we define *water_in* = (channel + surface + subsurface inflow + precipitation) and *water_out* = (infiltration + evaporation). Note that clear maxima were not present for all case studies for NSE (Fig. 6), but when present they are shown connected to the equivalent maxima for KGE.

Table 1: The wetland case study areas. Total tropical land area is approx. 56 000 000 km^2 (approx. 38% of total global land)

Site	Location	Surface area
Neotropics	23.5°S to 23.5°N, 110.4°W to 34.6°W	Approx. 18 000 000 km^2 land area (Malhi, 2010)
Amazon	The Central Amazon (Brazil, Colombia, Peru) 15.0°S to 7.0°N, 75.0°W to 47.0°W	Approx. 1 900 000 km^2 (Yamazaki et al., 2011; Gedney et al., 2019)
Pantanal	The Pantanal (Brazil, Bolivia, Paraguay) 22.0°S to 14.8°N, 61.1°W to 54.6°W	Varies up to 220 000 km^2 (Parker et al., 2018)
West Paleotropics	Tropical Africa and Arabia 23.5°S to 23.5°N, 17.6°W to 64.0°E	Approx. 21 000 000 km^2 land area
Niger Inland Delta	The Inner Niger Delta wetland (Mali) 13.6°N to 17.1°N, 5.2°W to 2.8°W	Varies up to 80 000 km^2 (Dadson et al., 2010; Bergé-Nguyen and Crétaux, 2015; Haque et al., 2020; Balek, 1977; Andersen et al., 2005)
Sudd	The Sudd (South Sudan) 4.5°N to 10.0°N, 28.0°E to 33.0°E	Varies up to 64 000 km^2 (Balek, 1977; Mohamed and Savenije, 2014; Sutcliffe and Parks, 1999; Tootchi et al., 2019), including the Bahr el Ghazal to the west and the Machar marshes to the east.
Congo	The Congo Cuvette Centrale (D. R. Congo, Congo-Brazzaville) 3.2°S to 3.6°N, 14.6°E to 25.2°E	Approx. 1 000 000 km^2 (Alsdorf et al., 2016; Betbeder et al., 2014; Balek, 1977)
Okavango	The Okavango Wetlands (Botswana) 24.0°S to 16.0°S, 19.0°E to 27.0°E	Varies up to 38 000 km^2 (the main delta NW of Maun varies up to 22 000 km^2 and the Makgadikgadi pans are an additional 16 000 km^2) (Milzow et al., 2009; Wolski et al., 2012)..
East Paleotropics	India to New Guinea 23.5°S to 23.5°N, 64.0°E to 153.5°E	Approx. 17 000 000 km^2 land area
Tonlé Sap	Tonlé Sap wetland (Cambodia) 11.6°N to 13.6°N, 103.0°E to 105.1°E	Varies up to 16 000 km^2 (Sithirith, 2015)

Table 2: Efficiency metrics widely used in flood model assessment and forecast verification (Knoben et al., 2019). In all equations, Q = flow variable (e.g. discharge) over time steps $t=1,..,T$. Subscripts "obs" and "sim" refer to observed and model-predicted values, respectively, $\mu_{obs} = \overline{Q_{obs}}$ is the observation mean and $\sigma_{obs} = \sqrt{\frac{1}{N-1}\sum_t(Q_{obs}(t) - \overline{Q_{obs}})^2}$ is the standard

465   deviation (and similarly for μ_{sim} and σ_{sim}) and r is the Pearson correlation coefficient between observed and simulated values.

Evaluation metric	Equation	Description
Nash-Sutcliffe efficiency (NSE) [*]	$NSE = 1 - \dfrac{\sum_t\left(Q_{sim}(t) - Q_{obs}(t)\right)^2}{\sum_t(Q_{obs}(t) - \overline{Q_{obs}})^2}$	Standard thresholds for NSE (but see Supp. Info): 1.0 = Perfect alignment > 0.5 = Good alignment (Knoben et al., 2019; Decharme et al., 2012) (although some other authors specify >0.6, e.g. Martínez-De La Torre et al. (2019)) 0.0 = No predictive skill (mean of observations provides as good an estimate as simulations) < 0.0 = Increasing divergence between simulations and observations Note that in this study points of very low inundation (dry areas *sensu* Bernhofen et al. (2018)) and very high inundation (permanent lakes and reservoirs) were removed before calculating NSE (because of the requirement to have at least some flow variability for the calculation), therefore our NSE values were slightly lower than usual. Our analysis rests on relative rather than absolute values of NSE, so our results are unaffected by this, but for clarity of comparison between sites we have used a consistent colour scale on all NSE plots based on the standard thresholds.
Kling-Gupta efficiency (KGE) [*, **]	$KGE = 1$ $- \sqrt{(r-1)^2 + \left(\dfrac{\sigma_{sim}}{\sigma_{obs}} - 1\right)^2 + \left(\dfrac{\mu_{sim}}{\mu_{obs}} - 1\right)^2}$	Standard thresholds for KGE: 1.00 = Ideal model performance > $(1 - \frac{1}{\sqrt{2}} =)$ 0.29 = Good performance (Knoben et al., 2019) $(1 - \sqrt{2} =)$ -0.41 = No predictive skill (mean of observations provides as good an estimate as simulations; n.b. negative values above this threshold still indicate that a model is an improvement over the mean flow benchmark) (Knoben et al., 2019) < -0.41 = Increasing divergence between simulations and observations Note that in this study points of very low inundation (dry areas *sensu* Bernhofen et al. (2018)) and very high inundation (permanent lakes and reservoirs) were removed before calculating KGE (because of the requirement to have at least some flow variability for the calculation), therefore our KGE values were

slightly lower than usual. Our analysis rests on relative rather than absolute values of KGE, so our results are unaffected by this, but for clarity of comparison between sites we have used a consistent colour scale on all KGE plots based on the standard thresholds.

[*] n.b. Both NSE and KGE are uncorrected for the magnitude of the variability of the observations σ_{obs}, (see Suppl. Info).

[**] n.b. KGE without the penalty terms (in μ and σ) reduces simply to Pearson's correlation coefficient $= \frac{cov(Q_{sim}(t), Q_{obs}(t))}{\sigma_{sim}\sigma_{obs}} = \frac{1}{N-1}\frac{\sqrt{\sum_t\left((Q_{sim}(t)-\overline{Q_{sim}})(Q_{obs}(t)-\overline{Q_{obs}})\right)}}{\sigma_{sim}\sigma_{obs}}$.

470

Aires, F., Prigent, C., Fluet-Chouinard, E., Yamazaki, D., Papa, F., and Lehner, B.: Comparison of visible and multi-satellite global inundation datasets at high-spatial resolution, Remote Sens Environ, 216, 427-441, 2018.

475   Alsdorf, D., Beighley, E., Laraque, A., Lee, H., Tshimanga, R., O'Loughlin, F., Mahe, G., Dinga, B., Moukandi, G., and Spencer, R. G. M.: Opportunities for hydrologic research in the Congo Basin, Reviews of Geophysics, 54, 378-409, 10.1002/2016RG000517, 2016.

Andersen, I., Dione, O., Jarosewich-Holder, M., and Olivry, J.-C.: The Niger River Basin: A Vision for Sustainable Management, The International Bank for Reconstruction and Development / The World Bank, Washington, D.C., 2005.

Arduini, G., Fink, G., and Martínez-de la Torre, A.: End-user-focused improvements and descriptions of the advances introduced between
480   the WRR tier1 and WRRtier2, 2017.

Balek, J.: Hydrology and water resources in tropical Africa, Elsevier, Amsterdam, Netherlands1977.

Bates, P. D., Horritt, M. S., and Fewtrell, T. J.: A simple inertial formulation of the shallow water equations for efficient two-dimensional flood inundation modelling, Journal of Hydrology, 387, 33-45, 10.1016/j.jhydrol.2010.03.027, 2010.

Beck, H. E., van Dijk, A. I. J. M., de Roo, A., Dutra, E., Fink, G., Orth, R., and Schellekens, J.: Global evaluation of runoff from 10 state-
485   of-the-art hydrological models, Hydrology and Earth System Sciences, 21, 2881-2903, 10.5194/hess-21-2881-2017, 2017.

Bergé-Nguyen, M. and Crétaux, J.-F.: Inundations in the Inner Niger Delta: Monitoring and Analysis Using MODIS and Global Precipitation Datasets, Remote Sens-Basel, 7, 2127-2151, 2015.

Bernhofen, M. V., Whyman, C., Trigg, M. A., Sleigh, P. A., Smith, A. M., Sampson, C. C., Yamazaki, D., Ward, P. J., Rudari, R., Pappenberger, F., Dottori, F., Salamon, P., and Winsemius, H. C.: A first collective validation of global fluvial flood models for major
490   floods in Nigeria and Mozambique, Environmental Research Letters, 13, 2018.

Best, M. J., Pryor, M., Clark, D. B., Rooney, G. G., Essery, R. L. H., Ménard, C. B., Edwards, J. M., Hendry, M. A., Porson, A., Gedney, N., Mercado, L. M., Sitch, S., Blyth, E., Boucher, O., Cox, P. M., Grimmond, C. S. B., and Harding, R. J.: The Joint UK Land Environment Simulator (JULES), model description – Part 1: Energy and water fluxes, Geoscientific Model Development, 4, 677-699, 10.5194/gmd-4-677-2011, 2011.

495   Betbeder, J., Gond, V., Frappart, F., Baghdadi, N. N., Briant, G., and Bartholome, E.: Mapping of Central Africa Forested Wetlands Using Remote Sensing, Ieee J-Stars, 7, 531-542, 2014.

Bierkens, M. F. P.: Global hydrology 2015: State, trends, and directions, Water Resources Research, 51, 4923-4947, 10.1002/2015WR017173, 2015.

Blyth, E. M., Martinez-de la Torre, A., and Robinson, E. L.: Trends in evapotranspiration and its drivers in Great Britain: 1961 to 2015,
500   Prog Phys Geog, 43, 666-693, 10.1177/0309133319841891, 2019.

Clark, D. B., Mercado, L. M., Sitch, S., Jones, C. D., Gedney, N., Best, M. J., Pryor, M., Rooney, G. G., Essery, R. L. H., Blyth, E., Boucher, O., Harding, R. J., Huntingford, C., and Cox, P. M.: The Joint UK Land Environment Simulator (JULES), model description – Part 2: Carbon fluxes and vegetation dynamics, Geoscientific Model Development, 4, 701-722, 10.5194/gmd-4-701-2011, 2011.

Clark, M. P., Bierkens, M. F. P., Samaniego, L., Woods, R. A., Uijlenhoet, R., Bennett, K. E., Pauwels, V. R. N., Cai, X., Wood, A. W.,
505   and Peters-Lidard, C. D.: The evolution of process-based hydrologic models: historical challenges and the collective quest for physical realism, Hydrology and Earth System Sciences, 21, 3427-3440, 10.5194/hess-21-3427-2017, 2017.

Clark, M. P., Fan, Y., Lawrence, D. M., Adam, J. C., Bolster, D., Gochis, D. J., Hooper, R. P., Kumar, M., Leung, L. R., Mackay, D. S., Maxwell, R. M., Shen, C. P., Swenson, S. C., and Zeng, X. B.: Improving the representation of hydrologic processes in Earth System Models, Water Resources Research, 51, 5929-5956, 10.1002/2015WR017096, 2015.

510   d'Orgeval, T., Polcher, J., and de Rosnay, P.: Sensitivity of the West African hydrological cycle in ORCHIDEE to infiltration processes, Hydrology and Earth System Sciences, 12, 1387-1401, DOI 10.5194/hess-12-1387-2008, 2008.

Dadson, S. J., Ashpole, I., Harris, P., Davies, H. N., Clark, D. B., Blyth, E., and Taylor, C. M.: Wetland inundation dynamics in a model of land surface climate: Evaluation in the Niger inland delta region, J Geophys Res-Atmos, 115, 10.1029/2010jd014474, 2010.

Dadson, S. J., Blyth, E. M., Clark, D. B., Davies, H., Ellis, R. J., Lewis, H. W., Marthews, T. R., and Rameshwaran, P.: A reduced-
515   complexity model of fluvial inundation with sub-grid representation of floodplains, Hydrology and Earth System Science, submitted 2021.

Dadson, S. J., Hall, J. W., Murgatroyd, A., Acreman, M., Bates, P., Beven, K., Heathwaite, L., Holden, J., Holman, I. P., Lane, S. N., O'Connell, E., Penning-Rowsell, E., Reynard, N., Sear, D., Thorne, C., and Wilby, R.: A restatement of the natural science evidence concerning catchment-based 'natural' flood management in the UK, P Roy Soc a-Math Phy, 473, 10.1098/Rspa.2016.0706, 2017.

Davison, B., Pietroniro, A., Fortin, V., Leconte, R., Mamo, M., and Yau, M. K.: What is Missing from the Prescription of Hydrology for
520   Land Surface Schemes?, Journal of Hydrometeorology, 17, 2013-2039, 10.1175/Jhm-D-15-0172.1, 2016.

Decharme, B., Alkama, R., Papa, F., Faroux, S., Douville, H., and Prigent, C.: Global off-line evaluation of the ISBA-TRIP flood model, Clim Dynam, 38, 1389-1412, 2012.

Dutra, E., Balsamo, G., Calvet, J., Minvielle, M., Eisner, S., Fink, G., Peβenteiner, S., Orth, R., Burke, S., van Dijk, A., Polcher, J., Beck, H., and Martínez-de la Torre, A.: Report on the current state-of-the-art Water Resources Reanalysis, 2015.

525   Dutta, D., Herath, S., and Musiake, K.: Flood inundation simulation in a river basin using a physically based distributed hydrologic model, Hydrological Processes, 14, 497-519, Doi 10.1002/(Sici)1099-1085(20000228)14:3<497::Aid-Hyp951>3.0.Co;2-U, 2000.

Fassoni-Andrade, A. C., Fan, F. M., Collischonn, W., Fassoni, A. C., and de Paiva, R. C. D.: Comparison of numerical schemes of river flood routing with an inertial approximation of the Saint Venant equations, Rbrh-Rev Bras Recur, 23, 10.1590/2318-0331.0318170069, 2018.

530   Fink, G. and Martínez-de la Torre, A.: Documentation on the improvements in hydrologic simulations from V2 EO datasets, 2017.

Froend, R. H., Horwitz, P., and Sommer, B.: Groundwater Dependent Wetlands, in: The Wetland Book II: Distribution, Description, and Conservation, edited by: Finlayson, C. M., Milton, G. R., Prentice, R. C., and Davidson, N. C., Springer, Dordrecht, Netherlands, 345-356, 10.1007/978-94-007-6173-5_246-1, 2016.

Gedney, N., Huntingford, C., Comyn-Platt, E., and Wiltshire, A.: Significant feedbacks of wetland methane release on climate change and
535   the causes of their uncertainty, Environmental Research Letters, 14, 10.1088/1748-9326/Ab2726, 2019.

Gerbeaux, P., Finlayson, C. M., and van Dam, A. A.: Wetland Classification: Overview, in: The Wetland Book: I: Structure and Function, Management and Methods, edited by: Finlayson, C. M., Everard, M., Irvine, K., McInnes, R. J., Middleton, B. A., van Dam, A. A., and Davidson, N. C., Springer Netherlands, Dordrecht, 1-8, https://doi.org/10.1007/978-90-481-9659-3_329, 2018.

Gumbricht, T., Román-Cuesta, R. M., Verchot, L. V., Herold, M., Wittmann, F., Householder, E., Herold, N., and Murdiyarso, D.:
540   Tropical and Subtropical Wetlands Distribution (2.0) [dataset], 2017.

Haque, M. M., Seidou, O., Mohammadian, A., and Djibob, A. G.: Development of a time-varying MODIS/ 2D hydrodynamic model relationship between water levels and flooded areas in the Inner Niger Delta, Mali, West Africa, Journal of Hydrology, 30, https://doi.org/10.1016/j.ejrh.2020.100703, 2020.

Hewlett, J. D.: Principles of Forest Hydrology, University of Georgia Press, Athens, Georgia1982.

545   Hidayat, H., Vermeulen, B., Sassi, M. G., Torfs, P. J. J. F., and Hoitink, A. J. F.: Discharge estimation in a backwater affected meandering river, Hydrology and Earth System Sciences, 15, 2717-2728, 2011.

Hoch, J. M. and Trigg, M. A.: Advancing global flood hazard simulations by improving comparability, benchmarking, and integration of global flood models, Environmental Research Letters, 14, 034001, 2019.

Hu, S. J., Niu, Z. G., and Chen, Y. F.: Global Wetland Datasets: a Review, Wetlands, 37, 807-817, 10.1007/s13157-017-0927-z, 2017.

550   IPCC: Climate Change 2014: The Physical Science Basis, Cambridge University Press, U.K.2014.

Junk, W. J., Piedade, M. T. F., Schongart, J., Cohn-Haft, M., Adeney, J. M., and Wittmann, F.: A Classification of Major Naturally-Occurring Amazonian Lowland Wetlands, Wetlands, 31, 623-640, 10.1007/s13157-011-0190-7, 2011.

Junk, W. J., An, S. Q., Finlayson, C. M., Gopal, B., Kvet, J., Mitchell, S. A., Mitsch, W. J., and Robarts, R. D.: Current state of knowledge regarding the world's wetlands and their future under global climate change: a synthesis, Aquat Sci, 75, 151-167, 2013.

555   Knoben, W. J. M., Freer, J. E., and Woods, R. A.: Technical note: Inherent benchmark or not? Comparing Nash-Sutcliffe and Kling-Gupta efficiency scores, Hydrology and Earth System Sciences, 23, 4323-4331, 10.5194/hess-23-4323-2019, 2019.

Lehner, B. and Döll, P.: Development and validation of a global database of lakes, reservoirs and wetlands, Journal of Hydrology, 296, 1-22, 10.1016/j.jhydrol.2004.03.028, 2004.

Lewis, H. W., Sanchez, J. M. C., Arnold, A., Fallmann, J., Saulter, A., Graham, J., Bush, M., Siddorn, J., Palmer, T., Lock, A., Edwards,
560   J., Bricheno, L., Martinez-de La Torre, A., and Clark, J.: The UKC3 regional coupled environmental prediction system, Geoscientific Model Development, 12, 2357-2400, 10.5194/gmd-12-2357-2019, 2019.

Lewis, H. W., Sanchez, J. M. C., Graham, J., Saulter, A., Bornemann, J., Arnold, A., Fallmann, J., Harris, C., Pearson, D., Ramsdale, S., Martinez-de la Torre, A., Bricheno, L., Blyth, E., Bell, V. A., Davies, H., Marthews, T. R., O'Neill, C., Rumbold, H., O'Dea, E., Brereton, A., Guihou, K., Hines, A., Butenschon, M., Dadson, S. J., Palmer, T., Holt, J., Reynard, N., Best, M., Edwards, J., and Siddorn, J.: The
565   UKC2 regional coupled environmental prediction system, Geoscientific Model Development, 11, 1-42, 10.5194/gmd-11-1-2018, 2018.

Liang, J. Y. and Liu, D. S.: A local thresholding approach to flood water delineation using Sentinel-1 SAR imagery, Isprs J Photogramm, 159, 53-62, 10.1016/j.isprsjprs.2019.10.017, 2020.

Malhi, Y.: The carbon balance of tropical forest regions, 1990-2005, Curr Opin Env Sust, 2, 237-244, 2010.

Maltby, E. and Barker, T.: The Wetlands Handbook, Blackwell, 10.1002/9781444315813, 2009.

570   Marthews, T. R., Blyth, E. M., Martinez-de la Torre, A., and Veldkamp, T. I. E.: A global-scale evaluation of extreme event uncertainty in the eartH2Observe project, Hydrology and Earth System Sciences, 24, 75-92, 10.5194/hess-24-75-2020, 2020.

Marthews, T. R., Jones, R. G., Dadson, S. J., Otto, F. E. L., Mitchell, D., Guillod, B. P., and Allen, M. R.: The Impact of Human-Induced Climate Change on Regional Drought in the Horn of Africa, J Geophys Res-Atmos, 124, 4549-4566, 10.1029/2018JD030085, 2019.

Martínez-de la Torre, A., Blyth, E. M., and Weedon, G. P.: Using observed river flow data to improve the hydrological functioning of the
575   JULES land surface model (vn4.3) used for regional coupled modelling in Great Britain (UKC2), Geoscientific Model Development, 12, 765-784, 10.5194/gmd-12-765-2019, 2019.

Melton, J. R., Wania, R., Hodson, E. L., Poulter, B., Ringeval, B., Spahni, R., Bohn, T., Avis, C. A., Beerling, D. J., Chen, G., Eliseev, A. V., Denisov, S. N., Hopcroft, P. O., Lettenmaier, D. P., Riley, W. J., Singarayer, J. S., Subin, Z. M., Tian, H., Zurcher, S., Brovkin, V., van

580 Bodegom, P. M., Kleinen, T., Yu, Z. C., and Kaplan, J. O.: Present state of global wetland extent and wetland methane modelling: conclusions from a model inter-comparison project (WETCHIMP), Biogeosciences, 10, 753-788, 10.5194/bg-10-753-2013, 2013.

Miguez-Macho, G. and Fan, Y.: The role of groundwater in the Amazon water cycle: 1. Influence on seasonal streamflow, flooding and wetlands, J Geophys Res-Atmos, 117, 2012.

Milzow, C., Kgotlhang, L., Bauer-Gottwein, P., Meier, P., and Kinzelbach, W.: Regional review: the hydrology of the Okavango Delta, Botswana-processes, data and modelling, Hydrogeol J, 17, 1297-1328, 2009.

585 Mitsch, W. J. and Gosselink, J. G.: The value of wetlands: importance of scale and landscape setting, Ecol Econ, 35, 25-33, Doi 10.1016/S0921-8009(00)00165-8, 2000.

Mitsch, W. J. and Gosselink, J. G.: Wetlands, 5th, Wiley, Hoboken, New Jersey2015.

Mohamed, Y. and Savenije, H. H. G.: Impact of climate variability on the hydrology of the Sudd wetland: signals derived from long term (1900-2000) water balance computations, Wetl Ecol Manag, 22, 191-198, 10.1007/s11273-014-9337-7, 2014.

590 Moomaw, W. R., Chmura, G. L., Davies, G. T., Finlayson, C. M., Middleton, B. A., Natali, S. M., Perry, J. E., Roulet, N., and Sutton-Grier, A. E.: Wetlands In a Changing Climate: Science, Policy and Management, Wetlands, 38, 183-205, 2018.

Papa, F., Prigent, C., Durand, F., and Rossow, W. B.: Wetland dynamics using a suite of satellite observations: A case study of application and evaluation for the Indian Subcontinent, Geophysical Research Letters, 33, 2006.

Papa, F., Prigent, C., Aires, F., Jimenez, C., Rossow, W. B., and Matthews, E.: Interannual variability of surface water extent at the global
595 scale, 1993–2004, Journal of Geophysical Research: Atmospheres, 115, 2010.

Parker, R. J., Wilson, C., Bloom, A. A., Comyn-Platt, E., Hayman, G., McNorton, J., Boesch, H., and Chipperfield, M. P.: Exploring Constraints on a Wetland Methane Emission Ensemble with GOSAT Satellite Observations, in prep. 2020.

Parker, R. J., Boesch, H., McNorton, J., Comyn-Platt, E., Gloor, M., Wilson, C., Chipperfield, M. P., Hayman, G. D., and Bloom, A. A.: Evaluating year-to-year anomalies in tropical wetland methane emissions using satellite CH4 observations, Remote Sens Environ, 211,
600 261-275, 10.1016/j.rse.2018.02.011, 2018.

Pham-Duc, B., Prigent, C., Aires, F., and Papa, F.: Comparisons of Global Terrestrial Surface Water Datasets over 15 Years, Journal of Hydrometeorology, 18, 993-1007, 10.1175/Jhm-D-16-0206.1, 2017.

Pires, J. M. and Prance, G. T.: The Vegetation Types of the Brazilian Amazon, in: Amazonia, edited by: Prance, G. T., and Lovejoy, T. E., Pergamon Press, Oxford, UK, 109-145, 1985.

605 Prigent, C., Jimenez, C., and Bousquet, P.: Satellite-Derived Global Surface Water Extent and Dynamics Over the Last 25 Years (GIEMS-2), J Geophys Res-Atmos, 125, 2020.

Prigent, C., Papa, F., Aires, F., Rossow, W. B., and Matthews, E.: Global inundation dynamics inferred from multiple satellite observations, 1993-2000, J Geophys Res-Atmos, 112, 10.1029/2006jd007847, 2007.

Prigent, C., Rochetin, N., Aires, F., Defer, E., Grandpeix, J. Y., Jimenez, C., and Papa, F.: Impact of the inundation occurrence on the deep
610 convection at continental scale from satellite observations and modeling experiments, J Geophys Res-Atmos, 116, 2011.

R Core Team: R: A language and environment for statistical computing (4.0.2), R Foundation for Statistical Computing [code], 2020.

Ramsar: An Introduction to the Ramsar Convention on Wetlands, Ramsar Convention Secretariat, Gland, Switzerland, 2016.

Robinson, E. L., Blyth, E. M., Clark, D. B., Finch, J., and Rudd, A. C.: Trends in evaporative demand in Great Britain using high-resolution meteorological data, Hydrology and Earth System Sciences, 21, 1189-1224, 10.5194/hess-2015-520, 2017.

615 Saunois, M., Stavert, A. R., Poulter, B., Bousquet, P., Canadell, J. G., Jackson, R. B., Raymond, P. A., Dlugokencky, E. J., Houweling, S., Patra, P. K., Ciais, P., Arora, V. K., Bastviken, D., Bergamaschi, P., Blake, D. R., Brailsford, G., Bruhwiler, L., Carlson, K. M., Carrol, M., Castaldi, S., Chandra, N., Crevoisier, C., Crill, P. M., Covey, K., Curry, C. L., Etiope, G., Frankenberg, C., Gedney, N., Hegglin, M. I., Hoglund-Isaksson, L., Hugelius, G., Ishizawa, M., Ito, A., Janssens-Maenhout, G., Jensen, K. M., Joos, F., Kleinen, T., Krummel, P. B., Langenfelds, R. L., Laruelle, G. G., Liu, L. C., Machida, T., Maksyutov, S., McDonald, K. C., McNorton, J., Miller, P. A., Melton, J. R.,
620 Morino, I., Muller, J., Murguia-Flores, F., Naik, V., Niwa, Y., Noce, S., Doherty, S. O., Parker, R. J., Peng, C. H., Peng, S. S., Peters, G. P., Prigent, C., Prinn, R., Ramonet, M., Regnier, P., Riley, W. J., Rosentreter, J. A., Segers, A., Simpson, I. J., Shi, H., Smith, S. J., Steele, L. P., Thornton, B. F., Tian, H. Q., Tohjima, Y., Tubiello, F. N., Tsuruta, A., Viovy, N., Voulgarakis, A., Weber, T. S., van Weele, M., van der Werf, G. R., Weiss, R. F., Worthy, D., Wunch, D., Yin, Y., Yoshida, Y., Zhang, W. X., Zhang, Z., Zhao, Y. H., Zheng, B., Zhu, Q., Zhu, Q. A., and Zhuang, Q. L.: The Global Methane Budget 2000-2017, Earth Syst Sci Data, 12, 1561-1623, 2020.

625 Schellekens, J., Dutra, E., Martinez-de la Torre, A., Balsamo, G., van Dijk, A., Weiland, F. S., Minvielle, M., Calvet, J. C., Decharme, B., Eisner, S., Fink, G., Florke, M., Pessenteiner, S., van Beek, R., Polcher, J., Beck, H., Orth, R., Calton, B., Burke, S., Dorigo, W., and Weedon, G. P.: A global water resources ensemble of hydrological models: the eartH2Observe Tier-1 dataset, Earth Syst Sci Data, 9, 389-413, 10.5194/essd-9-389-2017, 2017.

SimpleMaps: Basic World Cities Database (1.6), Pareto Software [dataset], 2019.

630 Sithirith, M.: The Governance of Wetlands in the Tonle Sap Lake, Cambodia, Journal of Environmental Science and Engineering B, 4, 331-346, 10.17265/2162-5263/2015.06.004, 2015.

Stacke, T. and Hagemann, S.: Development and evaluation of a global dynamical wetlands extent scheme, Hydrology and Earth System Sciences, 16, 2915-2933, 10.5194/hess-16-2915-2012, 2012.

635 Sterk, G., Sperna-Weiland, F., and Bierkens, M.: Guest Editorial: Special Issue on Global Hydrological Datasets for Local Water Management Applications, Water Resour Manag, 34, 2111-2116, 2020.

Sutcliffe, J. V.: Hydrology: a Question of Balance, International Association of Hydrological Sciences (IAHS) Special Publication, IAHS Press, Wallingford, UK2004.

Sutcliffe, J. V. and Parks, Y. P.: The Hydrology of the Nile, IAHS Special Publications 5, International Association of Hydrological Sciences (IAHS) Press1999.

640 Taylor, C. M.: Feedbacks on convection from an African wetland, Geophysical Research Letters, 37, 2010.

Taylor, C. M., Prigent, C., and Dadson, S. J.: Mesoscale rainfall patterns observed around wetlands in sub-Saharan Africa, Quarterly Journal of the Royal Meteorological Society, 144, 2118-2132, 10.1002/qj.3311, 2018.

Thirel, G., Andreassian, V., Perrin, C., Audouy, J. N., Berthet, L., Edwards, P., Folton, N., Furusho, C., Kuentz, A., Lerat, J., Lindstrom, G., Martin, E., Mathevet, T., Merz, R., Parajka, J., Ruelland, D., and Vaze, J.: Hydrology under change: an evaluation protocol to
645 investigate how hydrological models deal with changing catchments, Hydrolog Sci J, 60, 1184-1199, 2015.

Tootchi, A., Jost, A., and Ducharne, A.: Multi-source global wetland maps combining surface water imagery and groundwater constraints, Earth Syst Sci Data, 11, 189-220, 10.5194/essd-11-189-2019, 2019.

USEPA: Methods for Evaluating Wetland Condition: Wetlands Classification, Office of Water, U.S. Environmental Protection Agency, Washington, DC, 2002.

650 Vörösmarty, C. J., McIntyre, P. B., Gessner, M. O., Dudgeon, D., Prusevich, A., Green, P., Glidden, S., Bunn, S. E., Sullivan, C. A., Liermann, C. R., and Davies, P. M.: Global threats to human water security and river biodiversity, Nature, 467, 555-561, 2010.

Wheeler, B. D. and Shaw, S. C.: Wetland resource evaluation and the NRA's role in its conservation. 2. Classification of British wetlands, R&D Note, 378, National Rivers Authority, Bristol, UK, 106pp. pp.1995.

WMO: Statement on the state of the global climate in 2018, World Meteorological Organization, Geneva, Switzerland, 2019.

655 Wolski, P., Todd, M. C., Murray-Hudson, M. A., and Tadross, M.: Multi-decadal oscillations in the hydro-climate of the Okavango River system during the past and under a changing climate, Journal of Hydrology, 475, 294-305, 10.1016/j.jhydrol.2012.10.018, 2012.

Yamazaki, D., de Almeida, G. A. M., and Bates, P. D.: Improving computational efficiency in global river models by implementing the local inertial flow equation and a vector-based river network map, Water Resources Research, 49, 7221-7235, 10.1002/wrcr.20552, 2013.

Yamazaki, D., Oki, T., and Kanae, S.: Deriving a global river network map and its sub-grid topographic characteristics from a fine-
660 resolution flow direction map, Hydrology and Earth System Sciences, 13, 2241-2251, DOI 10.5194/hess-13-2241-2009, 2009.

Yamazaki, D., Kanae, S., Kim, H., and Oki, T.: A physically based description of floodplain inundation dynamics in a global river routing model, Water Resources Research, 47, 10.1029/2010wr009726, 2011.

Yamazaki, D., Sato, T., Kanae, S., Hirabayashi, Y., and Bates, P. D.: Regional flood dynamics in a bifurcating mega delta simulated in a global river model, Geophysical Research Letters, 41, 3127-3135, 10.1002/2014GL059744, 2014.

665 Zender, C. S.: Analysis of Self-describing Gridded Geoscience Data with netCDF Operators (NCO), Environmental Modelling & Software, 23, 4, 2008.

Zhang, Z., Zimmermann, N. E., Kaplan, J. O., and Poulter, B.: Modeling spatiotemporal dynamics of global wetlands: comprehensive evaluation of a new sub-grid TOPMODEL parameterization and uncertainties, Biogeosciences, 13, 1387-1408, 10.5194/bg-13-1387-2016, 2016.

670 Zhao, F., Veldkamp, T. I. E., Frieler, K., Schewe, J., Ostberg, S., Willner, S., Schauberger, B., Gosling, S. N., Schmied, H. M., Portmann, F. T., Leng, G. Y., Huang, M. Y., Liu, X. C., Tang, Q. H., Hanasaki, N., Biemans, H., Gerten, D., Satoh, Y., Pokhrel, Y., Stacke, T., Ciais, P., Chang, J. F., Ducharne, A., Guimberteau, M., Wada, Y., Kim, H., and Yamazaki, D.: The critical role of the routing scheme in simulating peak river discharge in global hydrological models, Environmental Research Letters, 12, 2017.

Zhou, X., Prigent, C., and Yamazaki, D.: Reasonable agreement and mismatch of land surface water area estimation between a global river
675 model and Landsat, in prep. 2020.

Zhou, X., Ma, W., Echizenya, W., and Yamazaki, D.: Uncertainty in flood frequency analysis of hydrodynamic model simulations, Natural Hazards and Earth System Sciences Discussions, 2020.